The Journal of Neuroscience, September 1989, 9(9): 3188–3208

Integration of Distributed Cortical Systems by Reentry: A Computer Simulation of Interactive Functionally Segregated Visual Areas

Leif H. Finkel[a] and Gerald M. Edelman

The Neurosciences Institute and The Rockefeller University, New York, New York 10021

A computer model based on visual cortex has been constructed to analyze how the operations of multiple, functionally segregated cortical areas can be coordinated and integrated to yield a unified perceptual response. We propose that cortical integration arises through the process of reentry—the ongoing, parallel, recursive signaling between separate maps along ordered anatomical connections. To test the efficacy of this reentrant cortical integration (RCI) model, we have carried out detailed computer simulations of 3 interconnected cortical areas in the striate and extrastriate cortex of the macaque. The simulated networks contained a total of over 222,000 units and 8.5 million connections.

The 3 modeled areas, called V_{OR}, V_{OC}, and V_{MO}, incorporate major anatomical and physiological properties of cortical areas V1, V3, and V5 but are vastly simplified compared with monkey visual cortex. Simulated area V_{OR} contains both orientation and directionally selective units; simulated area V_{MO} discriminates the direction of motion of arbitrarily oriented objects; and simulated area V_{OC} responds to both luminance and occlusion boundaries in the stimulus. Area V_{OC} is able to respond to illusory contours (Kanizsa, 1979) by means of the same neural architecture used for the discrimination of occlusion boundaries. This architecture also generates responses to structure-from-motion by virtue of reentrant connections from V_{MO} to V_{OC}. The responses of the simulated networks to these illusions are consistent with the perceptual responses of humans and other species presented with these stimuli. The networks also respond in a consistent manner to a novel illusion that combines illusory contours and structure-from-motion. The response synthesized to this combined illusion provides a strong argument supporting the need for a recursive reentrant process in the cortex.

Functional integration of the simulated areas in the RCI model were found to depend upon the combined action of 3 reentrant processes: (1) conflicting responses among segregated areas are competitively eliminated, (2) outputs of each area are used by other areas in their own operations, and (3) outputs of an area are "reentered" back to itself (through lower areas) and can thus be used iteratively to synthesize responses to complex or illusory stimuli. Transection of the reentrant connections selectively abolished these integrative processes and led to failure of figural synthesis.

The proposed model of reentry suggests a basis for understanding how multiple visual areas as well as other cortical areas may be integrated within a distributed system.

Recent studies of the visual system have shown that the visual cortex of higher animals is segregated into multiple distinct areas (Zeki, 1969; Allman and Kaas, 1971) that are interconnected by an extensive system of anatomical connections (Gilbert and Kelly, 1975; Tigges et al., 1977; Rockland and Pandya, 1979; Maunsell and Van Essen, 1983). Although the functional properties of these areas overlap considerably, each cortical area is, to a large extent, functionally specialized for the discrimination of a particular visual attribute such as shape, color, motion, or depth (Zeki, 1978; Livingstone and Hubel, 1988). A fundamental problem in early visual function is therefore to determine how the operations of these distributed cortical areas are coordinated and integrated to produce a coherent and unified response to objects in the stimulus domain. This problem is compounded by the requirement that the integrated system must respond to a wide range of signals, including partial, conflicting, or ambiguous stimuli.

Several models have addressed this problem of integrated cortical action. Marr (1982), for example, proposed a hierarchical model in which the visual cortex computes a series of successively abstracted "sketches" of the visual scene. Marr's model is deliberately not tied to cortical anatomy, however, and does not deal with the coordination of individual areas operating in parallel. More recently, several connectionist models (Ballard et al., 1983; Kienker et al., 1986) have emphasized the need for a distributed representation of cortical properties. These models perform specific visual tasks, including the formation of associations between different visual attributes (shape, color, etc.). However, they are primarily formal models based on analyses of the information-processing requirements of the tasks, and as such are difficult to relate directly to the nervous system.

In the reentrant cortical integration (RCI) model proposed here, the representation of the stimulus world remains distrib-

Received Nov. 2, 1988; revised Mar. 1, 1989; accepted Mar. 2, 1989.

We thank Dr. George N. Reeke, Jr. for advice and extensive help in implementation of the simulations. L.H.F. is Charles and Mildred Schnurmacher Fellow at The Neurosciences Institute. This work was supported in part by the Neurosciences Research Foundation, the Office of Naval Research, and Senator Jacob Javits Center for Excellence in Neuroscience Award USPHS NS-22789.

Simulations were conducted using the Cornell National Supercomputer Facility, a resource of the Center for Theory and Simulation in Science and Engineering at Cornell University, which is funded in part by the National Science Foundation, New York State, and the IBM Corporation and members of the Corporate Research Institute.

Correspondence should be addressed to Dr. Gerald Edelman, The Rockefeller University, Box 159, 1230 York Avenue, New York, NY 10021.

[a] Present address: Department of Bioengineering and David Mahoney Institute for Neurological Sciences, University of Pennsylvania, Philadelphia, PA 19104.

uted among multiple, functionally segregated areas. This is in accord with a fundamental constraint posed by the cortical anatomy, namely, that no single area receives a projection from all the specialized visual areas (Zeki and Shipp, 1988). Thus, in the absence of a convergent higher-level representation, integration is achieved in the RCI model by a *dynamic* process of reentrant signaling along interareal connections. We define reentry as the temporally ongoing, parallel, and recursive signaling between 2 or more mapped regions along ordered anatomical connections (Edelman, 1978, 1987).[1] It will be shown that reentry allows each region to use discriminations made by other regions (about borders, motion, etc.) for its own operations. In addition, reentry serves to resolve conflicts between the responses of the different areas. (A conflict is said to exist when the properties of the stimulus inferred from the responses of the various cortical regions, *taken separately,* are in disagreement, usually as a result of the different sources of input each area receives from a unitary stimulus.) Reentrant signaling obviates the need for a hierarchical structure, or a "sketch," and suggests instead a recursive set of interactions and correlations as the basis of integration in distributed systems (Mountcastle, 1978).

The present paper describes the results of an explicit test of the RCI model by large-scale simulations of several functionally segregated cortical areas. Such detailed computer simulations provide perhaps the only practical means to analyze explicitly the enormously complex interactions occurring among interconnected networks. We carried out simulations of 3 functionally specialized areas, V_{OR}, V_{MO}, and V_{OC}. V_{OR} is specialized for orientation selectivity, V_{MO} is specialized to respond to the direction of motion of an object regardless of the orientation of its edges, and V_{OC} is specialized for occlusion, which is one of the major monocular cues to depth (Stevens, 1981). The simulated areas are named for their *dominant* functional specializations. However, it is important to emphasize that most cells in each area display selectivities to several visual attributes (e.g., most cells in V_{OR} are both orientation and direction selective), and not all cells in an area demonstrate the dominant functional specialization. The 3 areas, V_{OR}, V_{OC}, and V_{MO} roughly correspond to cortical areas V1, V3, and V5 in the monkey, respectively. However, there is no strict or complete correspondence between simulated and real areas. Thus, as we will discuss below, in many ways V_{OC} resembles cortical area V2 as much as V3.

A central premise of the RCI model is that *the same reentrant connections* responsible for cortical integration also generate the early bases for a number of visual illusions. The Kanizsa triangle (Kanizsa, 1979), for example, which has illusory contour, brightness, and depth effects, indicates that illusory features constructed by the cortex interact in a consistent fashion across several submodalities. Such visual illusions, used either singly or in combination (van Tuijl, 1975; Nakayama and Silverman, 1986; Ramachandran, 1986), provide a severe test for any model of multiple functionally segregated areas. This is the case because, although it is trivial to design a network capable of giving responses corresponding to 1 or 2 such illusions, it is quite a difficult task to find a neural architecture capable of responding appropriately to a wide range of both normal and illusory stimuli.

In the present model, 2 particularly revealing classes of illusions are used as tests of integration—illusory contours and structure-from-motion. Illusory contours (variously called subjective, anomalous, or cognitive contours) have been suggested to arise from certain juxtapositions of local cues to occlusion (Coren, 1972; Gregory, 1972; Kanizsa, 1979). Indeed, simulations of the RCI model raise the possibility that responses to occluding stimuli, illusory contours, and structure-from-motion may all be mediated by different reentrant connections in the same neural architecture. The success of the simulations suggests that reentrant integration can provide an economical explanation for a wide range of psychophysical phenomena while taking into account an equally wide range of anatomical and physiological observations.

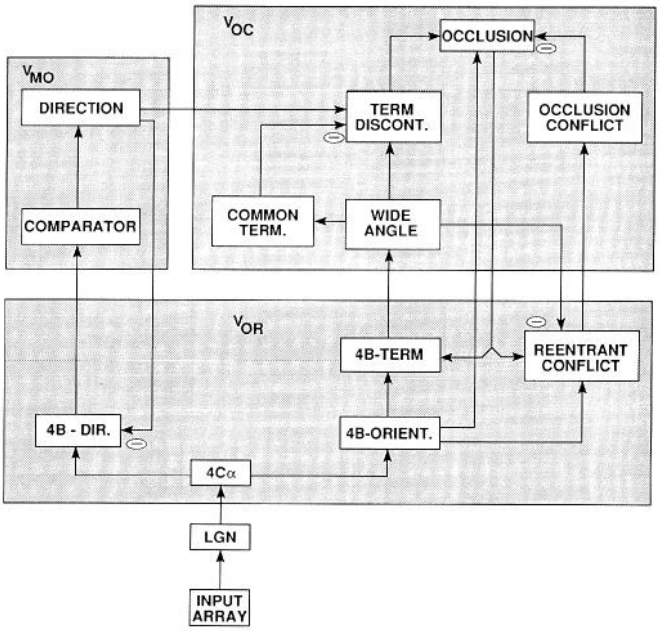

Figure 1. Schematic of network connectivity. Major connections between the simulated repertoires are indicated. Repertoires (*white boxes*) are named either according to their dominant function or to their closest analog in the CNS. The 3 shaded areas indicate the 3 simulated areas—V_{OR}, V_{OC}, V_{MO}—which are specialized for orientation, occlusion, and motion, respectively. Reentrant connections are indicated from the Direction repertoires of V_{MO} to "4B-Dir" of V_{OR}; from the Occlusion repertoires of V_{OC} to the "4B-Term" and Reentrant Conflict repertoires of V_{OR}; and from the Direction repertoires of V_{MO} to the Termination Discontinuity repertoires of V_{OC}. Note that these are not simple feedback loops; while only a single arrow is shown, reentry occurs from many units in parallel. All connections are excitatory unless indicated by a minus sign. Repertoire properties and connectivity details are given in the text and in Table 1.

Materials and Methods

We provide here a detailed description of the network connectivities and unit properties. The essential points are summarized in Figures 1 and 2 and Tables 1 and 2. It is important to emphasize that the particular functional properties modeled here (e.g., orientation or direction selectivity) are intended as exemplars: alternative mechanisms to generate

[1] The properties of reentry differ in a number of ways from those typically associated with "feedback" (Wiener, 1948). (1) Reentry is inherently parallel: it involves populations of interconnected units, not the recursion of a single scalar variable. (2) Reentry is distributed: each area simultaneously reenters to many other areas. The connections between areas are usually in register; however, they can be either convergent or divergent. (3) Reentry can occur between areas that are at the *same* heterarchical level, as well as between higher and lower levels in a system. (4) Reentry has a statistical or probabilistic nature: not all connections are used at all times. In addition, reentrant signaling can be either phasic or continuous over time. (5) Reentry can give rise to the construction of novel operations (discussed below) and is used more for correlation than for error correction or gain control.

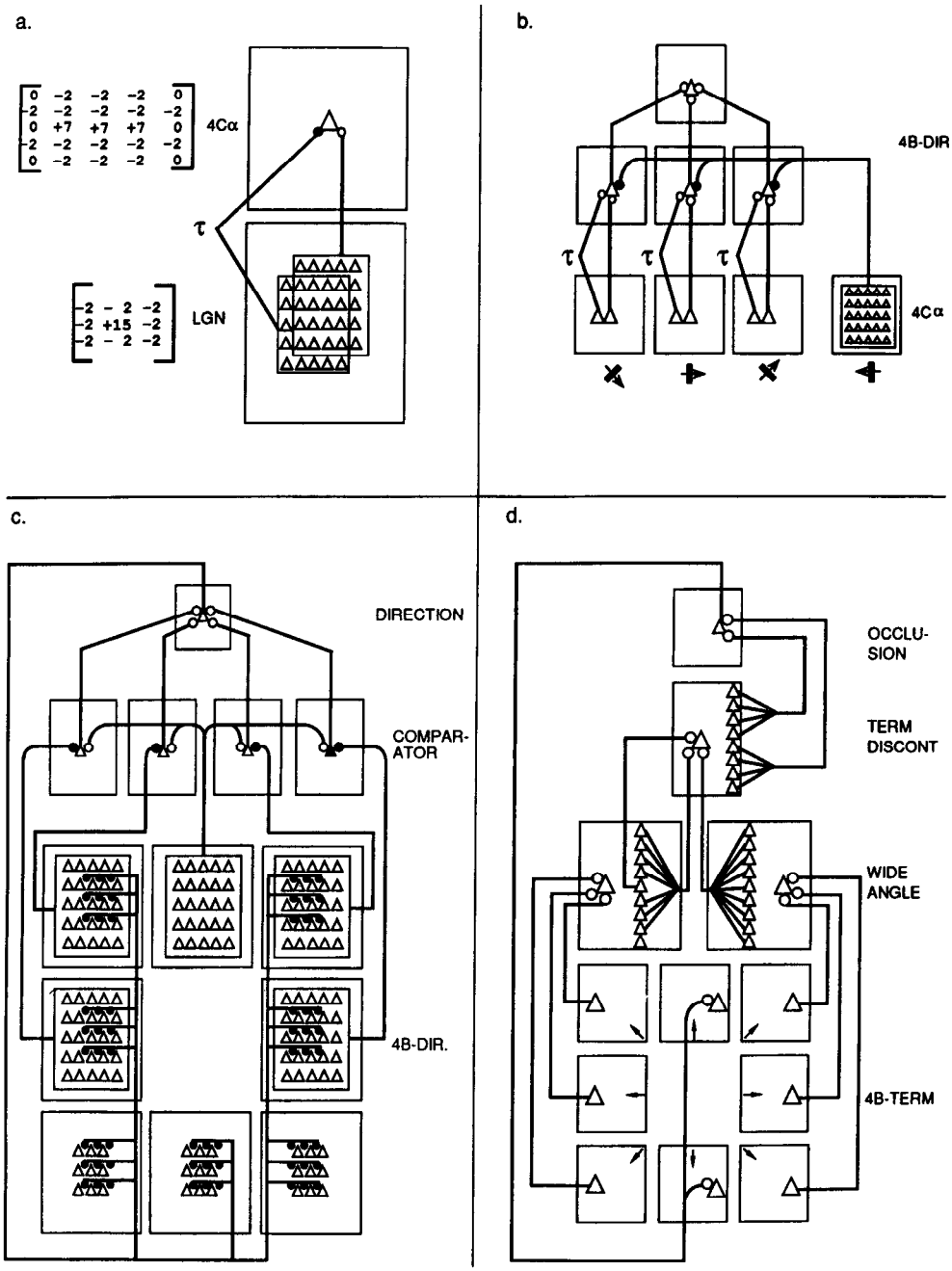

Figure 2. Details of network connectivity. *a,* Connections from "LGN" to "4Cα." The 2 matrices (*left*) give the connection strengths of inputs from the Input Array to an "LGN" unit (*bottom matrix*) and from the "LGN" to a "4Cα" unit (*top matrix*). Diagram at *right* shows geometry of connection scheme used to generate directional selectivity in "4Cα." Each "4Cα" unit receives excitation from a 5 × 5 unit region of the "LGN" (box containing 25 *triangles*)—the connection strengths are given by the (*top*) matrix at *left*. Each unit also receives connections (marked with τ) from a set of displaced "LGN" units. These connections activate a temporally delayed inhibitory mechanism (see text). The "4Cα" unit shown is selective for motion in a southwesterly direction. In this figure (*a–d*), *boxes* indicate repertoires, *triangles* indicate units, *lines* indicate connections, and *small circles* indicate synapses (*open,* excitatory; *closed,* inhibitory). The sizes of repertoires and units are adjusted for clarity—in the simulations, all repertoires contain 1024 units. *b,* Connections of a "4B-Dir" unit selective for eastward motion. Three repertoires containing a first type of "4B-Dir" unit (*middle row*) receive inputs from "4Cα" repertoires selective for motion in the southeasterly, easterly, and northeasterly directions, respectively (preferred direction indicated by *arrows*). Excitatory inputs are received from 2 adjacent "4Cα" units, one of which is displaced in the null direction (note positions of *triangles*) and acts through a temporally delayed mechanism (τ). The "4B-Dir" unit also receives inhibition from a 5 × 5 unit region in the "4Cα" repertoire selective for motion in the opposite (westerly) direction. These 3 "4B-Dir" units project to a second type of "4B-Dir" unit (*top*). *c,* The V_{MO} pathway. Shows connections received by a Direction unit selective for northward motion. Four comparator units compare responses to northward motion versus motion in a NE, NW, E, or W direction, respectively. Each comparator unit receives excitatory connections from a "4B-Dir" unit selective for northward motion and inhibitory connections from a 5 × 5 unit region in an adjacent "4B-Dir" repertoire (directional preferences indicated by relative position of panel; i.e., the preferred direction of the "4B-Dir" repertoire situated on the NW corner is NW). All 4 comparator repertoires project to the Direction unit (at least 3 inputs are needed to fire the unit). The direction unit provides reentrant connections back to 3 × 3 unit regions in all "4B-Dir" repertoires except for the repertoire selective for northward motion. This reentry yields a much sharper degree of directional selectivity (see Fig. 6). *d,* The ascending V_{OC} pathway. The diagram shows connections leading to an Occlusion unit selective for vertical boundaries. "4B-Term" units with orientations spanning 90° (preferred orientations indicated by *arrows*) send excitatory connections to Wide Angle repertoires. Wide Angle units from 2 repertoires with roughly opposite polarities (terminations roughly

these properties are possible, and a completely different set of properties could have as well been chosen. The central point of the RCI model is that *whatever* set of such functionally segregated properties is modeled, a reentrant mechanism will be necessary in order to achieve functional integration. The simulations are therefore based upon the assumption that a complete description of cortical cells and their connections is not necessary for the understanding of how integration takes place between cortical areas. The particular examples and mechanisms were chosen to illustrate this point.

All simulations were carried out on an IBM 3090 at the Cornell National Supercomputer Facility. Typical simulations required 12 megabytes of memory and CPU times averaged 12.3 sec/cycle. The simulations were carried out using a general-purpose cortical network simulator program (CNS) written by George N. Reeke, Jr. (Reeke and Edelman, 1987). This program allows the user to construct large-scale networks consisting of multiple types of units with detailed specification of the anatomical connectivity, as well as to emulate various electrical and chemical properties of synapses. The simulation package also allows stimulus objects of various sizes and shapes to be moved in specific ways across an input array.

Different *types* of simulated units are characterized by the source and distribution of their inputs and the operations (scales, thresholds, etc.) performed upon them. Multiple units of a given type compose a *repertoire,* and an *area* consists of multiple repertoires. Several major *pathways* within the system serially or reciprocally connect repertoires in several different areas. Unless otherwise stated, all connections between repertoires connect units at the topographically corresponding positions. All connections are generated at the start of a simulation, and the anatomy is thereafter fixed. There was no synaptic plasticity in the present simulations. The reader should refer to Figures 1 and 2 and Table 1 as the description of these elements proceeds.

All repertoires contain a multiple of 1024 (=32 × 32) units. The 3 simulated cortical areas (V_{OR}, V_{OC}, and V_{MO}) together contain 13 basic types of repertoires. There are 8 variants of each type of repertoire: the units in each variant differ with respect to their orientation or direction preferences (i.e., each variant contains units selective for one the 8 directions, N, NE, etc.). A total of 8,521,728 simulated synaptic connections are made among 222,208 units, for an average of 38 connections per unit (the range among different types is 2–350). In contrast, recent studies in the macaque (Peters, 1987) have estimated that Area 17 alone contains 155 million neurons (per hemisphere) with an average density of 120,000 neurons/mm^3. The density of synapses in macaque Area 17 is on the order of 4×10^8/mm^3, for an average across all cell types of approximately 3450 synapses per neuron. The relative paucity of connections received by units in the simulation undoubtedly reduces the variety and subtlety of their responses, but sufficient complexity remains to generate the phenomena of interest in these studies.

We have proposed elsewhere that the basic units of operation in the nervous system are neuronal groups (Edelman, 1978, 1987; Edelman and Finkel, 1984). These groups are strongly connected local populations of several hundred to several thousand neurons that share overlapping receptive fields and common response properties. Groups are proposed to play several critical roles in cortical function including the organization and maintenance of topographic maps (Pearson et al., 1987), and there are several lines of experimental evidence for their existence (Merzenich et al., 1988; Gray and Singer, 1989). We have recently simulated such groups and their temporal and reentrant properties in a system somewhat simpler than the present one (Sporns et al., 1989). However, since we are primarily concerned in the present simulations with short-term responses to direct sensory stimulation, we have omitted synaptic plasticity, thereby eliminating the main mechanism by which neuronal groups are formed and maintained (Pearson et al., 1987). Accordingly, in the interest of reducing the size of the computation, we have let simplified individual neuron-like units stand in for neuronal groups as the basic elements in our simulations. These units are designed to compensate for several properties that would, in a more extensive simulation, differ as a result of the presence of neuronal groups. Thus, for example, the units in the model have precisely ordered anatomical connections that compensate for the smaller "target" area of a cell compared to a group. (The variability of actual connectivity in the nervous system requires groups to overcome statistical instabilities.)

The properties of groups *in vivo* are best suited to study by multielectrode techniques or optical methods, but single-cell recordings nevertheless give an indication of group properties since most cells within a group will reflect the cooperative activity of the total group (Pearson et al., 1987). Thus, the responses of individual units in the present simulations should correspond, to a large extent, to the results of single-cell recordings in the cortex.

Physiological parameters

Despite the large number of units and connections in the model, a relatively small number of parameters controls the physiological properties of the simulation. Each unit is a simplified model neuron that nonlinearly sums inputs from other units. The output of a unit, which corresponds to the average firing rate of a single neuron, is given by

$$S_i(t) = \left[\sum_k w_k \left\{ \sum_j c_{ij} [S_j(t) - \theta_k] \right\}_{\mathrm{MIN}_k}^{\mathrm{MAX}_k} - \Theta \right], \qquad (1)$$

where $S_i(t)$ is the output of unit i at time t. w_k is a weighting factor on the relative efficacy of connections of class k (a class of connections is defined as those that come from the same type of unit). The first summation (over k) is over the different classes of connections received by a unit, and the second summation (over j) is over each connection of class k. c_{ij} is the synaptic weight of the connection from unit j to unit i, θ_k is a threshold that inputs of class k must exceed to have any postsynaptic effect,[2] and Θ is the unit-type specific firing threshold for unit i. The square brackets, [ ], denote an implicit thresholding scheme: $[x] = 0$ if $x < 0$, and $[x] = x$ otherwise. The curly brackets, { }, denote a separate threshold that is applied to the sum of all inputs from a given class of connections: $\{x\}^{\mathrm{MAX}} = \mathrm{MAX}$ if $x > \mathrm{MAX}$, and $\{x\}^{\mathrm{MAX}} = x$ otherwise. $\{x\}_{\mathrm{MIN}} = 0$ if $x < \mathrm{MIN}$ and $\{x\}_{\mathrm{MIN}} = x$ otherwise. These thresholding schemes are a simple formal means of representing some of the inherent nonlinearities involved in dendritic processing.

It is important to note that the physiological properties of all units in the simulation are specified by a small number of parameters: 1 parameter per unit-type (Θ), 4 connection-class parameters (w_k, θ_k, MAX_k, and MIN_k), and 1 connection-specific parameter (c_{ij}). In practice, only a subset of these parameters (and thresholds) is used in each type of unit. Furthermore, the values chosen for these parameters are identical among the vast majority of units and connections. For example, most units have $\theta_k = 0.1$. Moreover, only in the LGN and 4Cα repertoires are weights (the c_{ij}'s) assigned to individual connections (these weights are indicated in Fig. 2*A*). In all other repertoires of the simulation, the weights on the individual connections are the same—all units from the same class of connections are assigned $c_{ij} = +1$ or -1 depending on whether the connection is excitatory or inhibitory. This represents an enormous reduction in the number of parameters.

The values used for the 4 remaining parameters were all mutually dependent. In fact, all of the units used in the model can be grouped into 5 "physiological" classes defined by the particular relationships among the parameter values. These classes can be described by the basic operations they carry out: (1) simple weighted summation—small Θ, various values of w_k, MAX_k, and MIN_k, not used; (2) filter of weak activity—small Θ and moderate MIN_k; (3) comparator—small Θ and different w_k for excitatory versus inhibitory classes of inputs; (4) multiple *AND*—large Θ and MAX_k adjusted so that activation requires concurrent

[2] The purpose of thresholding each input was to eliminate low-level activity due to responses to nonoptimal stimuli (e.g., orientations more than 45° from the preferred orientation). *In vivo* such a threshold would also filter out low-level noise and the tails of decaying voltages. We have found that θ_k can be slightly increased or decreased without effect, but that the amplifications inherent in a reentrant system make such a filter useful, particularly in the absence of the intrinsic inhibitory mechanisms found in the cortex.

←

rightward or roughly leftward) and distributed along a vertical line all project to the same Termination Discontinuity (TD) unit. This unit also receives a connection from the one unit at the corresponding position in the Wide Angle repertoire (connection leaving vertical row of units from the left in the Wide Angle repertoire at *left*). All 3 types of inputs are required to fire the TD unit. This reflects the condition for occlusion (see text). Occlusion units receive connections from units distributed along a vertical line in the TD repertoire—one set of inputs from units at positions above the corresponding TD unit and another set from below. To be activated, the Occlusion unit requires inputs from both sets. Occlusion units then send excitatory reentrant connections back the "4B-Term" reentrant repertoires selective for vertical lines.

Table 1. Properties of the repertoires

Repertoire	Major property	Afferents	Efferents	Connectivity details
"LGN"	ON-Center, OFF-Surround	Input Array	"4Cα"	1 pixel excitatory center, 3 × 3 pixel inhibitory surround.
"4Cα"	Orientation selectivity	"LGN"	"4B-Dir" "4B-Orient"	5 × 5 connection matrix for horizontal and vertical orientations; 7 × 7 matrix for obliques. Temporally delayed inhibition in null direction.
"4B-Dir"	Directional selectivity	"4Cα" Direction	Comparator	Two types: first type gets excitatory inputs from 2 adjacent "4Cα" units, one input is temporally delayed and displaced in preferred direction. Also receives inhibition from 5 × 5 units in the "4Cα" repertoire selective for null direction. Second type sums inputs from 3 such units whose orientation preferences span 90° and reentrant connections from Direction repertoires.
"4B-Orient"	Orientation selectivity	"4Cα"	"4B-Term" Reentr. Confl. Occlusion	Excitatory inputs from 4 adjacent colinear units in "4Cα" and inhibition from surround. All 4 excitatory inputs are required to fire unit.
"4B-Term"	Orientation and polarity of line terminations	"4B-Orient"	Wide Angle	Local circuit excited by "4B-Orient" unit and inhibited by adjacent "4B-Orient" unit.
"4B-Term" (reentrant)	Same as "4B-Term"	Occlusion	Wide Angle	Similar to 4B-Term but on connections from Occlusion repertoires instead of "4B-Orient."
Reentrant Conflict	Responds to crossings of real and illusory contours	Occlusion "4B-Orient" Wide Angle	Occlusion Conflict	Excitatory connections from Occlusion and from the "4B-Orient" repertoires in the 3 most nearly orthogonal directions. Inhibitory inputs from orthogonally oriented "4B-Orient" repertoires and from Wide Angle repertoire.
Wide Angle	Broadens orientation selectivity	"4B-Term"	Term. Disc. Common Term.	1 excitatory input from 3 "4B-Term" repertoires with adjacent directional preferences (e.g., N, NE, NW)
Common Term. Detector	Detects whether lines with orientations within 90° terminate at a common locus	Wide Angle	Term. Disc.	Connections from 2 Wide Angle repertoires with adjacent orientation preferences. Both inputs required to fire unit.
Termination Discontinuity	Responds to line terminations consistent with an occlusion boundary	Wide Angle Common Term.	Occlusion	Connections from linear strips (2 × 87) of units in each of 2 Wide Angle repertoires with opposite polarities and from a single unit at corresponding position in one of the 2 Wide Angle repertoires. One inhibitory connection from Common Termination.
Direction Discontinuity	Responds to differential motion consistent with an occlusion boundary	Direction	Occlusion (motion)	Similar scheme to Termination Discontinuity repertoires but with inputs from Direction repertoires. Time constant of voltage decay is longer to allow short-term persistence of responses to moving objects.
Occlusion	Responds to real contours, occlusion borders, and illusory contours	Term. Disc. Occl. Confl. "4B-Orient"	Reentr. Confl.	60 bipolar excitatory connections from units distributed along a line in TD repertoire. Single inhibitory connection from Occlusion Conflict repertoire. Excitatory connections from "4B-Orient."
Occlusion (motion)	Responds to occlusion borders based on structure-from-motion	Dir. Disc.	"4B-Term" (reentrant)	Similar connectivity to Occlusion repertoires on inputs from Direction Discontinuity repertoires.

Table 1. Continued

Repertoire	Major property	Afferents	Efferents	Connectivity details
Occlusion Conflict	Generates illusory contours between conflicting points found by Reentrant Conflict repertoire	Reentrant Conflict	Occlusion	Similar connectivity to Occlusion repertoire but on inputs from Reentrant Conflict repertoires.
Comparator	Compares motion in adjacent directions	"4B-Dir"	Direction	5 × 5 unit excitation and 5 × 5 unit inhibition from "4B-Dir" repertoires with adjacent preferred directions. For each direction, there are 4 comparator units (e.g., N vs NE, N vs NW, N vs E, and N vs W).
Direction	Directional selectivity	Comparator	"4B-Dir" Dir. Disc.	Sums inputs from 4 comparator repertoires with same preferred direction; 3 inputs needed to fire unit.

inputs from at least 2 different classes of connections; (5) heterosynaptic—MIN_k for one set of connections set extremely high so that they are ineffective. Activation of another class of (heterosynaptic) inputs to the unit lowers MIN_k and makes the first set of connections functional (this is the mechanism used for directional selectivity—see below).

The actual values of the parameters used in all the simulations reported here are given in Table 2. It is important to stress that the exact values used for any of these parameters have little qualitative effect on the simulation as long as the *relative* values of the parameters are maintained. While changing the exact values does change the range of activity levels over which the unit can operate, such effects were not important in the present simulations since we only used stimuli of maximal contrast. We would expect cells *in vivo* to show properties allowing a maximum range of response.

Anatomical connectivity and response properties

In the following, we describe the connectivities and properties of the various repertoires and units included in the model. The rationale for the inclusion of each type of unit is, in some cases, deferred to the Results. An example of the normal operation of the networks (i.e., how the various types of units function together in a simulation) is described as the last entry of Materials and Methods, and together with Figures 1 and 2 provides a basic guide to the construction of the simulations. After reading the descriptions of Figures 1 and 2, the noncomputationally oriented reader may wish to skip to that exemplary description for a first reading.

Figure 1 presents a simplified schematic of the overall network connectivity with further details given in Table 1 and Figure 2. As shown in the figure, the connections between V_{OR}, V_{OC}, and V_{MO} follow an anatomical plan similar to that found in the magnocellular pathway in visual cortical areas V1, V3, and V5. In the monkey, these 3 areas constitute a particularly simple reentrant system: V3 and V5 are directly interconnected and, in addition, both receive connections from and anatomically reenter to the same cell layer (4B) in V1 (Zeki, 1971; Rockland and Pandya, 1979; Burkhalter et al., 1986; Zeki and Shipp, 1988).

In the model, stimuli of various sizes and shapes excite the elements of the Input Array (64 × 64 pixels) which corresponds to a drastically simplified retina. There is a single pathway from the Input Array through the "LGN" to "4Cα." "4Cα" projects to "4B," which contains several separate populations of units. "4B-Dir" units are directionally selective and are reentrantly connected to V_{MO}. "4B-Orient." units are orientation selective and provide input to "4B-Term" units, which are specialized for detecting line terminations and are reentrantly connected to V_{OC}. "4B-Orient." units also project to Reentrant Conflict units which, as discussed below, respond to conflicts in the responses to real and illusory contours (these units signal an internal inconsistency in the determined occlusion relationships of several adjacent surfaces).

The "LGN" and "4Cα." The "LGN" contains ON-center, OFF-surround units that receive inputs from 3 × 3 pixel regions of the Input Array. The strengths of these connections are shown in Figure 2*a*. We have not included any OFF-center LGN units, and for that reason, light stimuli on dark backgrounds have been used exclusively.

The orientation selectivity of "4Cα" units arises from the spatial pattern of the connections from the "LGN." As the role of intracortical inhibition in orientation selectivity is still controversial (Ferster, 1987), a version of the original Hubel and Wiesel (1962) feedfoward model was chosen for computational simplicity. Each "4Cα" unit receives excitatory inputs from an elongated (3 × 1 unit) region of the LGN and inhibitory inputs from 2 elongated (5 × 2) flanks. The connection strengths of the inputs (Fig. 2*a*) are adjusted so that units can be partially activated by lines whose orientations are within 45° of the preferred orientation. The square geometry of the underlying pixel matrix necessitates different inhibitory surrounds for obliquely oriented versus horizontal or vertically oriented units.

Directional selectivity in "4Cα" is achieved through a mechanism involving temporally delayed inhibition that emulates a delayed IPSP. Inhibitory inputs from the "LGN" (see Fig. 2*a*) produce a signal (meant to emulate an intracellular second messenger) that leads to hyperpolarization of the unit through the opening of simulated ion channels. The temporal delay in the inhibition (denoted by τ in Fig. 2*a*) is controlled by the time constants of the production and decay of this signal. As shown in Figure 2*a*, each "4Cα" unit receives 2 sets of inputs from the "LGN," one excitatory and one inhibitory. Directional selectivity depends upon the fact that the inhibitory units are shifted with respect to the excitatory inputs (the direction of the shift will turn out to be the null direction of the "4Cα" unit). In these simulations, the 2 sets of inputs were always shifted by 1 unit, and the temporal delay was always 1 cycle; however, the same mechanism can be used to generate a range of velocity sensitivities.

V_{MO} pathway

"4B-Dir" units. Starting with the "4B-Dir" units, the V_{MO} pathway transforms the selectivity of unit responses from a primary selectivity to orientation (found in "4Cα") to a primary selectivity to direction (found in the Direction repertoires). As shown in Figure 2*b*, there are 2 types of "4B-Dir" units. One type (Fig. 2*b*, center row) receives excitatory inputs from 2 adjacent "4Cα" units. Using a temporal delay mechanism similar to that in "4Cα," the "4B-Dir" unit is activated only if one of these inputs (τ in Fig. 2*b*) occurs within a fixed time window before the other input. Each "4B-Dir" unit also receives direct-acting inhibitory inputs from a 5 × 5 unit region in the "4Cα" repertoire whose directional selectivity is in the null direction; this null inhibition greatly enhances the directional selectivity.

Inputs from 3 of these units with orientation preferences spanning 90° are then subjected to a threshold and summated by a second type of "4B-Dir" unit (Fig. 2*b*, top). Summation over the 3 directions (NE, E, SE) assures that "4B-Dir" will detect lines moving eastward even if they are not of the preferred orientation for a given "4Cα" repertoire. Because of the nonlinearity of unit properties, this local circuit scheme

Table 2. Repertoire classification and parameter values

Type of unit	Operational class	Θ	No. of connections	Action	w_k[a]	θ_k	MIN_k	MAX_k
LGN	Connection Matrix	0.1	9	Mixed	1.0	0.1		
4Cα	Conn. Matrix and	0.1	25[b]	Mixed	1.5	0.1		
	Heterosynaptic		25	Mixed	3.0	0.1	16.0[c]	
4B-Dir	Heterosynaptic	0.1	1	Exc	1.5	0.1	6.0	
(type 1)			1	Exc	1.5	0.1	20.0[c]	
			25	Inh	20.0	0.0		
4B-Dir	Weighted Sum	0.1	3 × 1[d]	Exc	1.1	0.1		
(type 2)			63[e]	Inh	5.0	0.1		
4B-Orient	Multiple *AND*	0.99	4 × 1	Exc	5.0	0.1		0.32
			2 × 5	Inh	1.0	0.1		
4B-Term[f]	Comparator	0.1	1	Exc	10.0	0.0		
			1	Inh	15.0	0.0		
Common Term.	Multiple *AND*	0.95	6 × 1	Exc	1.0	0.1		0.94
Wide Angle	Weighted Sum	0.1	3 × 1	Exc	1.0	0.1	0.5	
			3	Exc	4.0	0.1		
			1	Inh	5.0	0.1		
Reentrant	Multiple *AND*	0.95	3 × 2	Exc	15.0	0.1		0.3
Conflict			2	Exc	15.0	0.0		0.94
			2 × 2	Inh	15.0	0.1		
			4 × 9	Inh	5.0	0.1		
Termination	Multiple *AND*	0.95	1	Exc	10.0	0.1		0.62
Discontinuity			2 × 87	Exc	60.0	0.1		0.32
			2 × 87	Exc	60.0	0.1		0.15
			1	Inh	5.0	0.1		
Direction	Multiple *AND*	0.95	1	Exc	1.0	0.1		0.94
Disc.[f]			7	Exc	20.0	0.1		0.94
Occlusion	Multiple *AND*	0.95	2 × 30	Exc	60.0	0.1		0.94
			1	Inh	5.0	0.1		
			4 × 1	Inh	30.0	0.0		
Occlusion	Multiple *AND*	0.95	2 × 5	Exc	20.0	0.1		0.94
(motion)			11	Inh	40.0	0.1		
Occlusion	Multiple *AND*	0.95	2 × 31	Exc	20.0	0.0		0.94
Conflict								
Comparator	Comparator	0.1	25	Exc	1.0	0.0		
			25	Inh	1.1	0.0		
Direction[f]	Multiple *AND*	0.96	4 × 1	Exc	5.0	0.0		0.47

[a] The program rescales w_k by (32/no. of connections)$^{1/2}$.
[b] Units tuned for oblique orientations have more connections.
[c] Activates temporally delayed inhibition.
[d] 3 × 1 denotes 3 classes of 1 connection each.
[e] Additional unit types used to collate reentry.
[f] Not all unit types involved in this repertoire are shown.

is not equivalent to a single unit that receives, thresholds, and sums the inputs from "4Cα." For example, in this scheme, excitation of units in different "4Cα" repertoires will not give rise to activation of "4B-Dir."

Comparator units. As shown in Figure 2*c*, the first repertoires in V_{MO} are the comparator repertoires. There are 4 comparator units for each direction (e.g., north); each unit is inhibited by motion in one of the 4 adjacent directions (e.g., NE, NW, E, and W). Each comparator unit receives excitation from a 5 × 5 unit region in the corresponding "4B-Dir" repertoire (Fig. 2*c* shows the comparator units selective for motion in a *northward* direction), and inhibition from a 5 × 5 unit region in one of the adjacent "4B-Dir" repertoires. Thresholds are adjusted so that each comparator unit is activated only if the responses to motion in its preferred direction exceed those to motion in the adjacent direction.

Direction units. The final stage in the V_{MO} pathway (Fig. 2*c*, top) consists of units that sum inputs from the 4 comparator units selective for motion in a particular direction. Thresholds are arranged so that inputs from at least 3 of the 4 sources are necessary to fire a unit. This represents a majority vote on the differential comparisons carried out by the comparator repertoires and signals that the response to motion in a given direction is stronger than in the adjacent directions.

V_{MO}-V_{OR} reentry. As shown in Figure 2*c*, outputs from each direction unit are reentered back to "4B-Dir" in V_{OR}. Each direction unit inhibits a 3×3 unit region in all "4B-Dir" repertoires except the one with the same directional preference. This arrangement tends to suppress activity in "4B-Dir" repertoires that does not correspond to the active V_{MO} repertoire.

The long-distance inhibitory connections used here are rare in the nervous system, but similar results can be obtained through a long-range excitation of local intrinsic inhibitory cells. Such a mechanism

was proposed by Singer (1977) in his model of the role of corticogeniculate connections in stereopsis. In addition, we have found several alternative schemes of reentrant connectivity that help generate directional selectivity. For instance, excitatory reentrant connections to "4B-Dir" units can be coupled with cross-orientation inhibition (Blakemore et al., 1970). Alternatively, reentry can originate from the comparator units instead of the directional units. Several such schemes generate roughly equivalent results.

V_{OC} pathway

The V_{OC} pathway detects and generates responses to occlusion boundaries. As shown in Figure 3*B*, an occlusion boundary can be defined by the *presence* of textures or lines of various orientations (either stationary or moving) that terminate along its extent *and* by the *absence* of textures or lines that extend across the boundary. Figure 3*C* indicates the local cues to occlusion present in the occluding squares stimulus of Figure 3*A*. The V_{OC} pathway initially responds to local cues consistent with an occlusion boundary, but continued responses depend upon the global consistency of these local cues (i.e., whether multiple local terminations can be linked up along an extended discontinuity or "fracture" line—as in Fig. 3, *C, D*). The same local cues that indicate the presence of occlusion boundaries are responsible for the generation of illusory contours. Figure 3*D* shows a classic illusory contour that depends upon the parallel terminations of lines from 2 abutting grids. Figure 3*E* shows how similar terminations (in this case of both straight lines and curved arcs) give rise to the illusory contours of the well-known Kanizsa triangle.

Cues that *rule out* the presence of an occlusion can be as important as cues *consistent with* occlusion. For example, although line terminations often indicate the presence of an occlusion, when 2 lines both terminate at the same point, forming a vertex (see Fig. 8*A* for an example), the probability that the terminating lines continue under an occluding surface is lessened and the salience of the cues is thus diminished. As we shall see, the V_{OC} system also checks (through reentry) that the occlusion boundaries it discriminates obey a number of self-consistency relationships. For example, 2 occluding boundaries should not cross each other, nor should an occluding boundary cross a real boundary. These physical inconsistencies are reflected by internal conflicts in the system that must be resolved to yield a consistent pattern.

"4B-Term" units. As local cues to occlusion, the V_{OC} pathway uses both line terminations and the differential motion of textures. "4B-Term" units detect line terminations due to an inhibitory end-region in their receptive fields. End-stopped receptive fields are found in simple cells of layer 4B (Gilbert, 1977), as well as in complex cells of layers 2 and 3 (see Discussion). However, unlike end-stopped cells in the striate cortex, "4B-Term" units have only one end-inhibitory region and are thus sensitive to the polarity of the termination (i.e., at which end of the line the termination is found).

Wide Angle units. Since lines can terminate at an occlusion boundary with a variety of orientations with respect to that boundary (see Fig. 3*B*), Wide Angle units sum inputs from "4B-Term" units whose preferred orientations span 90° (see Fig. 2*d*).

Termination Discontinuity units. Wide Angle units project to Termination Discontinuity (TD) units that detect local cues to occlusion. As shown in Figure 3*B*, these local cues consist of any of several terminating lines that approach the presumptive occlusion boundary from either side. In order to be activated, a TD unit must be activated by at least 3 inputs from the Wide Angle repertoires—and at least one of these inputs must correspond to line terminations of an opposite polarity to that of the other inputs (see Fig. 2*D*). All 3 types of inputs must, in addition, come from units distributed along a line in a Wide Angle repertoire (and this is assured by the geometry of the connections).

A separate population of TD units (referred to as Direction Discontinuity units) carries out a similar operation upon inputs from V_{MO} that signal the presence of a discontinuity in motion. Use of a single population of TD units to receive inputs from both V_{OR} and V_{MO} is not possible because activation of a TD unit requires a combination of inputs, and a single unit (of the simple type used here) cannot distinguish a valid combination that arises from one set of sources from partial combinations which arise from 2 different sets of sources. Direction Discontinuity units have a slower time decay for voltages allowing them to maintain responses to moving stimuli that have recently passed through the receptive field of the unit.

Occlusion units. Occlusion units respond to the actual location and course of an occlusion boundary. Each Occlusion unit receives connections, in a bipolar fashion, from 2 sets of TD units distributed in opposite directions along a common line (see Fig. 2*d*). To be activated, an Occlusion unit must receive inputs from both bipolar branches (i.e., both sets of TD units). This connection scheme ensures that a string of adjacent Occlusion units will be activated by an occlusion boundary.

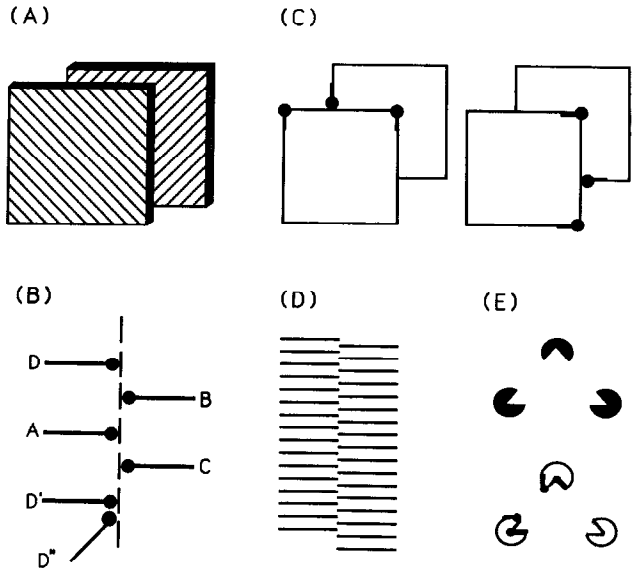

Figure 3. Occlusion and the scheme for generating illusory contours. *A*, Occlusion of one square object by another is indicated by perspective. *B*, Definition of an occlusion boundary. *Dashed vertical line* is the presumptive occlusion boundary; *circles* indicate line terminations. Occlusion boundary requires colinear terminations of at least 3 lines approaching border from both sides: i.e., *line A and* at least 2 of {*lines B, C,* and (*D* or *D'*)}. Lines approaching the boundary at an angle (*line D"*) are also allowed. These same conditions are used by the network to generate responses to illusory contours. *C*, Cues to occlusion boundaries in the figure shown in *A*. *Circles with stems* show line terminations that cue an occlusion boundary according to scheme shown in *B*. The figure at *left* shows the occlusion cues for the "top" occlusion boundary; figure at *right* shows cues for "right" occlusion boundary. *D*, Two abutting grids, one half-cycle out of phase, give rise to a vertical illusory contour at their line of intersection. Note the line terminations fulfill the conditions for occlusion given in *B*. The extreme left and right borders of the figure do not give rise to a vivid illusory contour. *E*, The classic Kanizsa (1979) triangle (*above*) and line terminations (*circles with stems*) giving rise to the illusory contour forming one side of the Kanizsa triangle (*below*). Corresponding terminations generate responses to other 2 sides. In this case, terminations of both lines and arcs are used—a generalization of scheme in *B*.

The ascending V_{OC} pathway shares several common features with an anatomical scheme proposed by Baumgartner and his colleagues (Peterhans et al., 1986) to account for the responses to illusory contours by units in Area V2 of rhesus monkeys. Although the details vary, both schemes use asymmetric end-inhibition, nonlinear summation of responses to colinear terminations, and a separate set of inputs to mediate responses to real contours. The model proposed here differs in several regards (see Discussion) that allow it to respond to a wider range of illusory objects, including illusory squares and triangles (Kanizsa, 1979).

The remaining repertoires and connections in the V_{OC} pathway (described below) deal with the elimination of false cues, the resolution of internal conflicts in generated responses, and the reentrant "recycling" back to V_{OR} of responses to occlusion boundaries determined in V_{OC}.

Common Termination units. Common Termination units respond to configurations in which 2 or more lines terminate at a common locus. These units sum inputs from Wide Angle units with identical receptive field locations and adjacent orientation preferences. Common Termination units directly inhibit TD units (see Fig. 1).

Reentrant Conflict units. Reentrant Conflict units respond to locations at which illusory contours cross real contours or other illusory contours. Reentrant Conflict units receive connections from 3 "4B-Orient." repertoires having orientations spanning 90° (in exactly the same manner

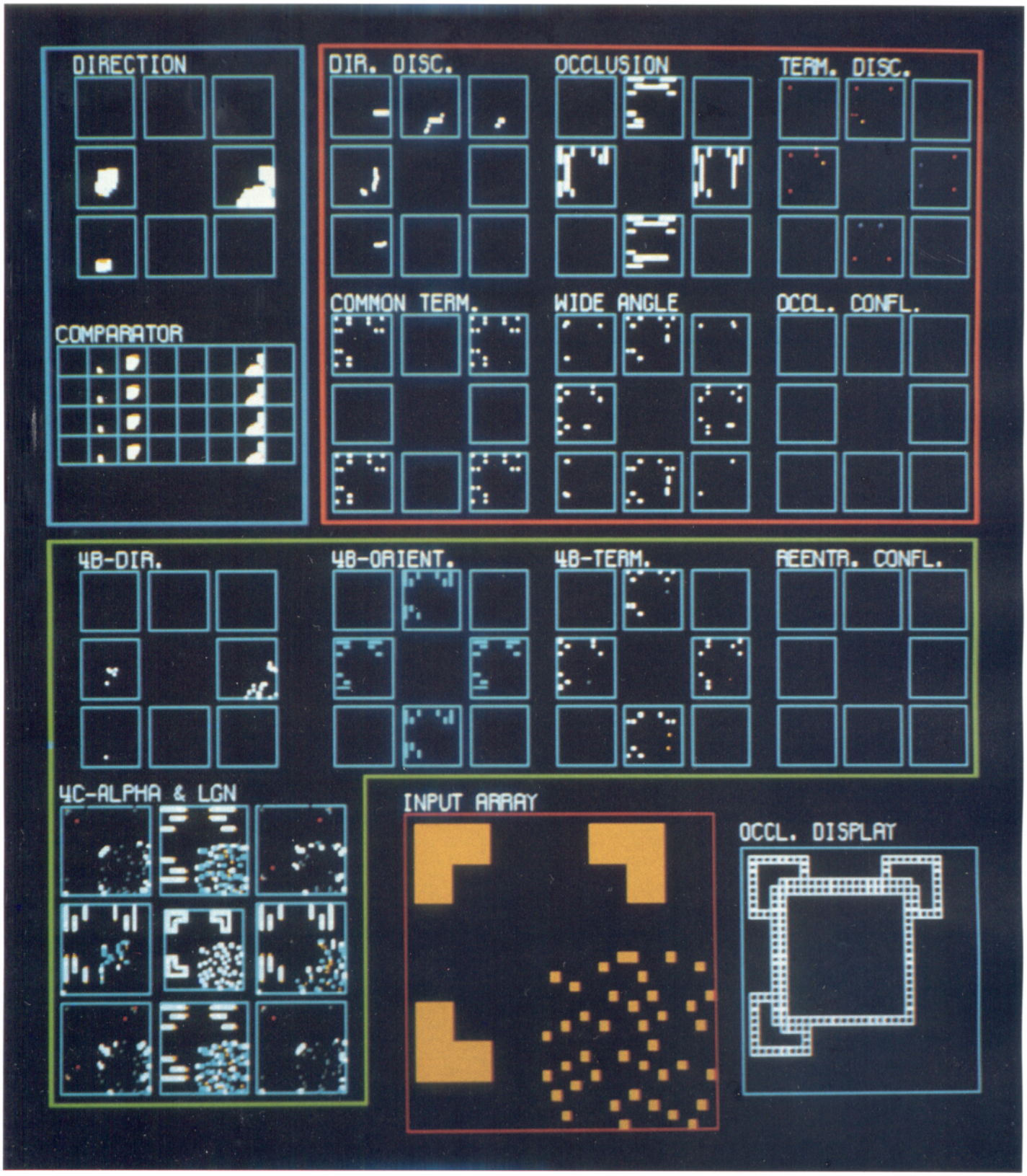

Figure 4. Actual network display seen on the computer screen. Responses of output units in the major repertoires (129 repertoires and 132,096 units) to the combined stimulus analyzed in Figure 10. *Square boxes* (*cyan*) indicate individual repertoires; *dots* within the repertoires indicate activity of units at the corresponding positions. *Large colored borders* demarcate repertoires belonging to the 3 simulated areas: green for V_{OR}, blue for V_{MO}, and orange for V_{OC}. Unit activity is color-coded from high to low in 5 colors: white, blue, green, yellow, and red. The 8 panels of each repertoire correspond to units segregated by orientation or direction preference: the position of each panel indicates the preference of its units (e.g., units in *upper left* "4Cα" panel prefer 135° lines). *This convention is used in all following figures.* Activity in the Input Array due to the stimulus is shown at the bottom center (responses shown in yellow). Panel labeled "Occl. Display" (*bottom right*) shows (at larger scale, for clarity) the

as Wide Angle units) and, in addition, receive excitatory reentrant connections from Occlusion units. To be activated, each Reentrant Conflict unit requires at least one input from an Occlusion unit (illusory line) *and* one input from a "4B-Orient." unit (real line) with an overlapping receptive field. Reentrant Conflict units are also strongly inhibited by corresponding units in the Wide Angle repertoires: since illusory contours *always* join real contours at their terminations, conflicts at a termination are not to be counted.

Occlusion Conflict units. Occlusion Conflict units receive connections from Reentrant Conflict units in exactly the same manner that Occlusion units receive connections from the TD repertoires, and they generate responses to (illusory) contours between the points of conflict. The Occlusion Conflict units directly inhibit Occlusion units, thereby canceling (through reentry) responses to any segment of a generated illusory contour that was in conflict.

Recursive synthesis by reentry. A final V_{OC} reentrant pathway allows signals generated by illusory contours and structure-from-motion to be reentered back to V_{OR} and treated *as if* they were signals from real contours in the periphery entering via "4Cα." This recursion is a key property of reentry. A separate population of "4B-Term" units is used to receive inputs from Occlusion units. These "4B-Term" units then project to the Wide Angle units, thereby merging with the signal stream of the normal ascending V_{OC} pathway. This reentrant pathway allows contours generated through structure-from-motion from V_{MO} inputs to be used as termination cues for the generation of additional illusory contours. This is the basis of the mechanism underlying the recursive synthesis simulation experiments to be discussed below.

Normal operation of the networks

Figure 4 provides a glimpse of how the multiple repertoires function together. The displays show the activity in all of the major repertoires during one cycle of a reentrant synthesis experiment (see discussion of Fig. 10 for details). The degree of activation of each unit is indicated by the color of the dot at the corresponding position in the panel (see legend). The 8 panels of each repertoire (arranged in a square) show the activities of the units segregated according to orientation or directional preference (e.g., upper-left panel contains units preferring motion in the upper-left direction). The success of the design of each repertoire can be judged by comparing the locations of responding units in the repertoires to the pattern of activity that would be ideally derived from the stimulus in the input array (i.e., Do the orientation selective repertoires respond correctly to oriented lines? Do the termination detectors respond to the ends of appropriately oriented lines?). Note that, for clarity, units are displayed in uniform arrays (32 × 32 units); however, the topographic nature of the mapping would be preserved under various topological distortions, such as might exist *in vivo.*

The normal operation of the networks can be seen by comparing the activity patterns shown in Figure 4 to the connectivity diagrams of Figures 1 and 2. Note that the "LGN" repertoires have responded to the outlines of the stimulus objects (see Fig. 4) and that the "4Cα" and "4B-Orient" repertoires selectively respond to particular orientations of these lines. The 1 pixel dots in the stimulus are moved (see discussion of Fig. 10 for details) and the "4B-Dir" and Direction repertoires respond, in a selective fashion, to the direction of the motion. The Direction Discontinuity repertoires respond to borders between regions of differential motion. Responses to these borders are reentered back to "4B-Term," which detects the terminations of these borders as well as of line terminations in the 3 corner stimuli. The Wide Angle repertoires then sum these responses in the manner described above. The Termination Discontinuity repertoires have constructed responses to the occlusion cues (i.e., each active unit signals that the condition described in Fig. 3*B* is met), and the Occlusion repertoires have generated responses to the illusory contours, as well as to the real contours present.

The responses of all 8 Occlusion repertoires are superposed in the Occlusion Display (bottom right) to show that an illusory square can be synthesized from a combination of illusory contours and structure-from-motion (see Fig. 10 for discussion). Note that there are no responses in the Reentrant Conflict or Occlusion Conflict repertoires because no conflicts are present between generated illusory contours and the real contours present in the stimulus.

Results

We first demonstrate that the orientation and directional selectivities of the simulated units qualitatively resemble those found *in vivo.* We then examine the responses of the system to real contours and occlusion boundaries and to various stimuli that, when presented to human subjects, produce illusory contours, structure-from-motion, and a novel combined illusion. Finally, we use these illusions to test the integrative properties of the system in both the presence and absence of reentrant connections. Note that for all simulations reported here, both the anatomy of the system and the values of the physiological parameters for the units (see Table 2) remain unchanged.

Functional properties of the networks

Orientation selectivity

Figure 5*A* shows the orientation selectivity of several different repertoires. Five oriented lines (each 6 × 1 pixels long) were presented, in turn, at orientations spaced 45° apart and were moved at 1 pixel/cycle (the preferred velocity) in the preferred direction. The averaged activity of units over 10 trials is plotted as a function of orientation, with the preferred orientation arbitrarily plotted at 0°. Units in the LGN respond equally well to all orientations, as expected from their circularly symmetric receptive fields (see Fig. 2*a*). Units in "4Cα" (curve labeled V_{OR}) show the emergence of orientation selectivity, with responses falling off by 50% at approximately 40°. Units in the Direction repertoires (curve labeled V_{MO}) are much less sharply tuned for orientation. The orientation selectivity of the "4B-Dir" and Comparator units (not shown) is similar to that of the Direction units; the orientation selectivities of units in the other repertoires of V_{OR} and V_{OC} are similar to that of "4Cα."

The broadness of the orientation tuning curves is determined by the weighting of the connection strengths on the spatially ordered inputs to these units (see Fig. 2*A*). Choice of the connection strengths was governed by 2 considerations: (1) to avoid the possibility of activation by lines that are orthogonal to the preferred orientation (by just nipping the edge of the excitatory center) and (2) to allow significant overlap in the response of units with adjacent orientation preferences (i.e., with 45°). This last consideration implies that a single unit cannot signal the orientation of a line; rather, a population response is required.

Figure 5, *B, C,* shows the directional selectivity of different stages in the V_{MO} pathway. We determined the response of units in the "4Cα" repertoires (Fig. 5*B*) and Direction repertoires (Fig. 5*C*) to moving lines of 3 different orientations (each 6 × 1 pixels long). Each line was moved in the 8 directions indicated (N, NE, etc.) at a speed of 1 pixel per iteration (horizontal and vertical movements) or 1.414 pixels per iteration (movements in oblique directions). Note the sharper directional selectivity of the Direction units (Fig. 5*C*) compared with that of the "4Cα" units (Fig. 5*B*). In "4Cα" there is stronger response to an op-

←

topographically superposed responses of units in all 8 Occlusion repertoires. The stimulus consisted of 3 aligned corner elements and 2 regions of random dots that were moved in different directions (see Fig. 10 and text for details) to generate borders due to structure-from-motion. Through the action of its reentrant circuits, the networks use both structure-from-motion and illusory contour cues to synthesize a response to an illusory square.

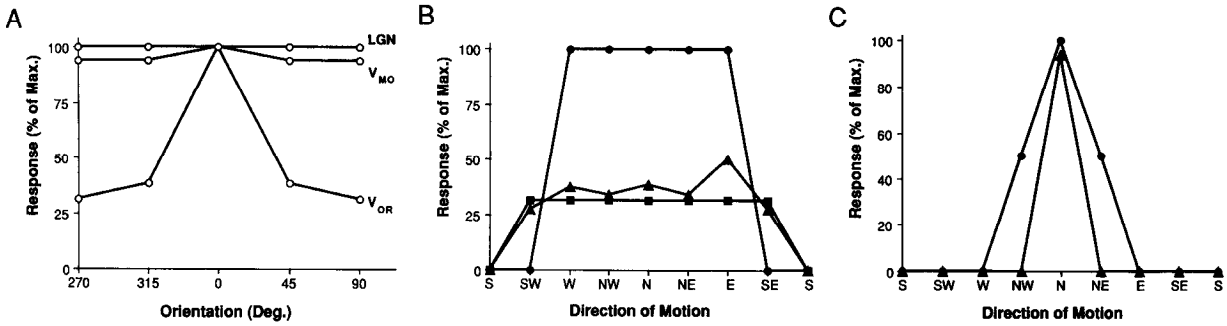

Figure 5. Orientation and directional tuning curves. *A,* Orientation tuning curves of units in the "LGN," V_{OR}, and V_{MO}. Response of typical units (averaged over 10 trials) to various orientations of a 6 × 1 pixel line moved at 1 pixel/cycle in the preferred direction (responses are normalized to maximum response of the unit). Note sharp tuning in V_{OR}, poor tuning in V_{MO}, and absence of tuning in "LGN." Curve labeled V_{OR} was from a "4Cα" unit, and curve labeled $V_{MO}$was from a Direction unit. *B,* Directional selectivity of "4Cα" units. Response (as percentage of maximum response) to a 6 × 1 pixel line moved in various directions (N, NE, etc.) of a "4Cα" unit whose preferred orientation was 0° and preferred direction was northward. The 3 curves plot responses to lines oriented at 0° (*circles*), 45° (*triangles*), and 90° (*squares*). Note that "4Cα" responds well to lines of the preferred orientation moved in a wide range of directions. *C,* Directional selectivity of Direction units. Response of a Direction unit whose preferred direction was northward to same stimuli as in *B.* Orientation of lines indicated as above. Curve obtained for 90° oriented line was exactly the same as curve shown for 45° line. Note that these units respond well to lines moving in the preferred direction regardless of their orientation.

timally oriented line moving in a nonoptimal direction than to a nonoptimally oriented line moving in the preferred direction. Thus, "4Cα" is primarily orientation selective and only secondarily direction selective. On the other hand, as can be seen from Figure 5*C,* Direction units are primarily direction selective and only secondarily orientation selective. Thus, the directional selectivity of the V_{MO} pathway shares a qualitative similarity to that found *in vivo* (Albright, 1984; Movshon et al., 1985).

Figure 6 shows the pattern of activation in the repertoires of "4Cα," "4B-Dir," and Direction repertoires to a moving random dot stimulus. The panels on the right in Figure 6 show the response to this stimulus when the reentrant connections from V_{MO} to V_{OR} have been eliminated. The stimulus consisted of 1 pixel dot generated at random positions over the Input Array and moved 1 pixel per iteration. Dots in the central third of the display were moved due south, while those in the left and right outer thirds of the display were moved due north. New arbitrarily placed dots were continually introduced at appropriate edges of the display so that the distribution of dots was at all times spatially homogeneous.

This figure uses the same convention for displaying repertoire activities as was used in Figure 4. The 8 boxes arranged in a square configuration show the activity of units in the 8 variants of each repertoire, with the relative position of each box indicating the preferred direction of that repertoire (i.e., the upper-left box shows the repertoire whose preferred direction is directed at 135°). A dot in the box indicates that the unit at the corresponding position in the repertoire is active, and the size of the dot indicates the degree of activation. Thus, by viewing the pattern of activation in the boxes and comparing the responses to the stimulus pattern, one can immediately judge the fidelity of the network responses.

As shown at the top center of Figure 6, after 4 cycles, only units in the central third of the *south* Direction repertoire are active, and only units in the outer thirds of the *north* Direction repertoire are active. There is no activity in any of the other Direction repertoires. Through the reentrant connections, this activity pattern is communicated back to the 4B-Dir repertoires. Thus, the true direction of motion of a moving random dot pattern is determined in only a few cycles of iteration. This pattern of activity is stable as long as the stimulus is maintained. In the *absence* of reentry (right panels), a number of units in both the "4B-Dir" and Direction repertoires show incorrect responses to the direction of motion of the random dots. In effect, "closing the loop" between V_{MO} and V_{OR} selects that set of units linked through the pathway whose combined primary and secondary selectivities lead to the most vigorous response. Note that the responses of "4Cα" are nearly identical in the 2 cases (since "4B-Dir" is the earliest repertoire affected by reentry; see Fig. 1).

Other simulations (not shown) demonstrate that the V_{MO} pathway with reentry can distinguish fields of dots moving in any 2 different directions (45° or more apart). In addition, the dividing line between the motion fields can have any arbitrary orientation or can constitute the boundary of an arbitrarily shaped region. This directional selectivity of the V_{MO} repertoires is crucial to the extraction of structure-from-motion, as will be shown below.

Generation of responses to illusory contours

Figure 7 shows the responses of the V_{OC} pathway to occlusion and illusory contour stimuli as well as to several control stimuli. In Figure 7*A,* responses to an illusory vertical "line" are generated from a stimulus consisting of 2 horizontal gratings ½ cycle out of phase. Figure 7*B* shows a control stimulus in which the terminations of the 2 gratings overlap so as to destroy the illusion of occlusion. As can be seen, the network does not generate responses to illusory contours in this case. Figure 7, *A, B,* contains an implicit control in that no responses to illusory contours are made at the extreme left or right edges of the gratings. Since terminations only approach these borders from one side, they do not meet the criteria for occlusion boundaries that were defined in reference to Figure 3*B.* It was in order to account for this perceptual phenomenon (that an illusory contour is not perceived at the edge of a grid) that "4B-Term" units were constructed with asymmetric end-inhibition (see Materials and Methods). Note also that, as in Figure 4, the "Occlusion Display" panel is solely intended for diagnostic use: these units do not provide input to any other repertoire in the simulation.

Figure 7*C* shows the responses generated to a stimulus that

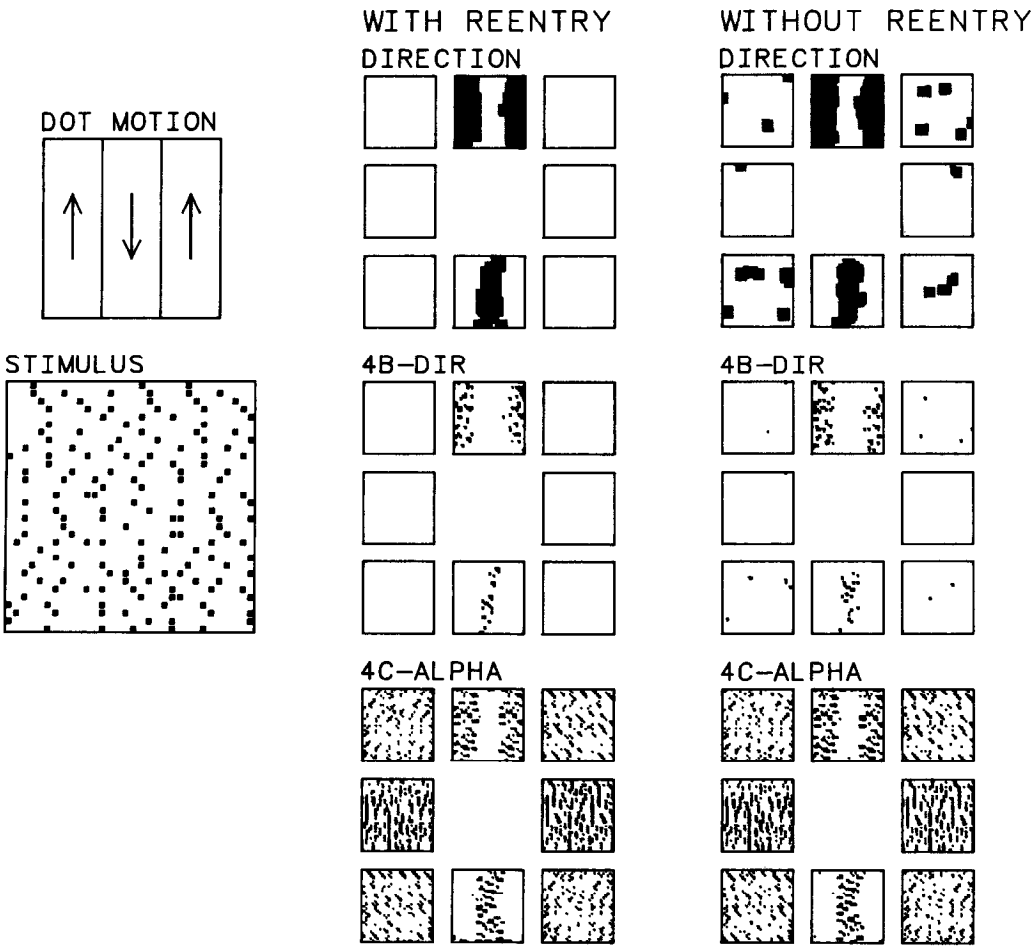

Figure 6. Responses to differentially moving random dots. Responses of all units in the "4Cα," "4B-Dir," and Direction repertoires (in the presence and absence of reentry) are shown after 4 cycles of a moving random dot pattern. Stimulus (at *left*) consisted of 1 pixel randomly placed dots. Dots in center third of display were moved southward, those in outer thirds were moved northward (panel labeled "Dot Motion") at 1 pixel/cycle. Panels are arranged by directional preference according to convention (see Fig. 4). The larger receptive fields of Directional cells are manifested by the number of cells responding to a single stimulus dot. "4Cα" units show a degree of directional selectivity, but many units selective for (what are in this case) incorrect directions (e.g., NE, NW, etc.) are active as well. The "4B-Dir" and Direction repertoires respond much more selectively to the direction of motion. Reentry leads to more accurate directional discrimination in that only units selective for the correct direction respond. Without reentrant connections (*right*), a number of Direction units respond incorrectly to dot motion. The responses of units in "4Cα" are nearly identical with or without reentry, since "4B-Dir" is the most peripheral repertoire to receive reentrant connections from V_{MO}.

is perceived by humans as an illusory square. The Occlusion repertoires have generated responses to the 4 sides of the illusory square (these responses arise on the first cycle of stimulation). The boundaries of this illusory square arise from local cues to occlusions given by the 4 corner objects [which are perceived by humans as small squares, but we do not study this "amodal completion" (Kanizsa, 1979) part of the problem]. The 2 examples of Figure 7, *A, C,* are particularly challenging for a network implementation since, in Figure 7*C,* the illusory contours are generated *parallel* to colinear lines in the stimulus, and in Figure 7*A* the contours are generated *perpendicular* to the lines of the stimulus. However, in both cases, it is terminations of line segments that are the key to the occlusion. Many other variants of these 2 stimuli can be dealt with by the model; note in particular that Figure 7*C* is closely related to the well-known Kanizsa triangle (Kanizsa, 1979).

Finally, Figure 7*D* shows a *normal* 2-dimensional stimulus that is perceived by humans as showing a central square occluding 2 other surfaces. The occlusion boundaries are discriminated by the V_{OC} system, i.e., only the borders of the central "occluding" square are detected. In this particular stimulus, the occlusion boundaries coincide with real luminance boundaries (the boundaries of the central square are both occlusion borders *and* luminance borders), and therefore, the responses to occlusion boundaries per se cannot be clearly distinguished in the display. For this reason, the normal ascending connections from the "4B-Orient." units to the Occlusion units (see Fig. 1) were cut before performing this simulation. In the presence of these connections, the occlusion repertoires respond to the occlusion boundaries in the same manner as seen here; in addition, the connections from the "4B-Orient." repertoires allow the Occlusion repertoires to respond to all of the real luminance contours in the stimulus. (Thus, the pattern of response in the "Occlusion Display" panel would look identical to the stimulus.) Through the use of a number of other stimuli, we have found that the V_{OC} system is successful in picking out occluding boundaries in a wide (but not all-inclusive) range of geometrical configurations.

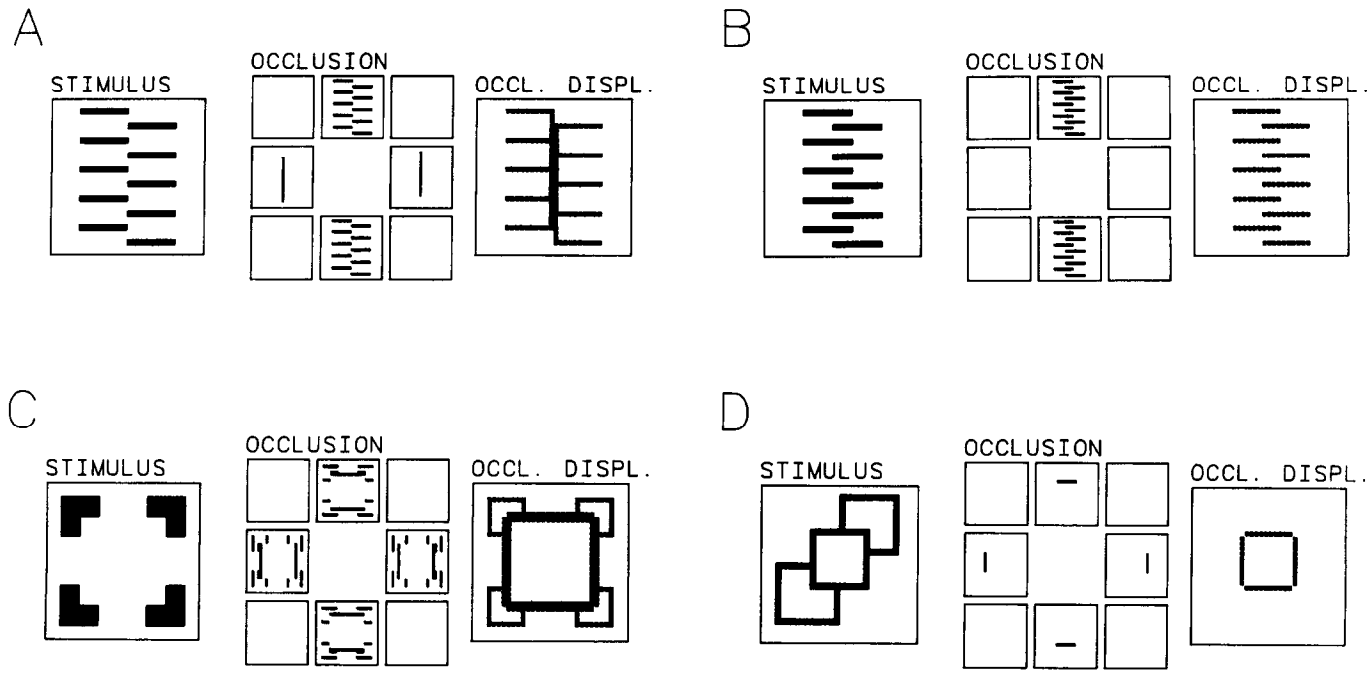

Figure 7. Generation of illusory contours. *A,* Response of occlusion repertoires (*center panels*) to an abutting grid stimulus (*left*) after 1 cycle of stimulation. Occlusion repertoires are arranged by orientation preference according to convention of Figure 4. Panel labeled "Occl. Displ." shows (at a larger scale, for clarity) the superposed responses of all 8 Occlusion repertoires. Note responses to both the real (horizontal) lines as well as the illusory (vertical) contour. *B,* Responses to a control stimulus in which terminations of the grids overlapped. There are no illusory contour responses. *C,* Classic illusory square stimulus. On first cycle of presentation, responses are generated to the edges of the 4 corner stimuli, as well as to the 4 illusory contours making up the square. *D,* Central square occluding 2 other squares. Connections from "4B-Orient" to Occlusion repertoires were cut in order to more clearly show responses to occlusion boundaries (in this stimulus, occlusion and real borders are superposed). Only the edges of the central square are discriminated as occlusion borders.

Conflict and V_{OC} reentry

The reentrant connections of the V_{OC} system can act to *rule out* an occlusion boundary because of false cues or conflicts with other boundaries—real or illusory. An example of a false cue is shown in Figure 8*A,* in which 4 right-angled vertices terminate along a common vertical line. The Common Termination units (see above) are sensitive to such terminations and act to prevent the local cues from activating the Termination Discontinuity repertoires. Thus, as is seen in Figure 8*A* (center), with the connections between Common Termination units and TD units intact, no responses to illusory contours are generated in the Occlusion repertoires. However, as shown in the right of the figure, in the absence of these connections, the false cues to termination give rise to responses to a vertical illusory contour in the Occlusion repertoires. These latter responses do not correspond to the perception of the stimulus as seen by human observers.

A second type of conflict is shown in Figure 8*B,* in which the "illusory square" stimulus of Figure 7*C* is modified so that a rectangular object crosses the path of one vertical illusory contour. Figure 8*B* shows the effect of the reentrant circuit that connects Occlusion → Reentrant Conflict → Occlusion Conflict → Occlusion repertoires (see Fig. 1). The normal action of the ascending V_{OC} pathway generates responses to the illusory contours comprising the square. The Occlusion Conflict repertoires then generate a *second* illusory contour between the points at which the edges of the rectangle cross the illusory contour. The Occlusion Conflict units inhibit the Occlusion units responding to the occluded section of the illusory contour. Thus, through the inhibitory action of the reentrant circuit, the illusory contour is "censored" in the region of conflict with the real contour (see Fig. 8*B,* center). When the reentrant connections from Occlusion to Reentrant Conflict units are cut, as shown on the right of Figure 8*B,* this inhibitory "censoring" does not occur, and the occlusion relationships are not discriminated.

In other simulations (not shown), we have investigated the case in which an illusory square (such as that in Fig. 7*C*) has one illusory side crossed by a single (real) line. In this case, the reentrant pathways "censor" the illusory contour only at the one point of conflict.

Figure 8*C* shows a stimulus that serves as a control for the stimulus of Figure 7*C* and that, in doing so, illustrates some of the strengths and limitations of the present approach. In the figure, the elements of the illusory square stimulus of Figure 7*C* have been rearranged in such a way that human observers do not perceive an illusory square. Inspection of the stimulus reveals that line terminations consistent with an illusory square are present (just as in Fig. 7*C*), the difference being that in the present case, occlusion boundaries generated from these terminations cross the interior of the 4 inducing elements. As shown on the right of Figure 8*C,* in the absence of the Occlusion Conflict reentrant system, the illusory contours are generated to form an illusory square. With the reentrant connections intact (Fig. 8*C,* center), however, these illusory contours are censored between the borders of the 4 corner elements. Even with reentry, it can be seen that the illusory contours still remain within the interiors of the 4 corner elements. We have found alternative schemes that allow these remaining contours to be censored, but the example serves to illustrate the point that these "mag-

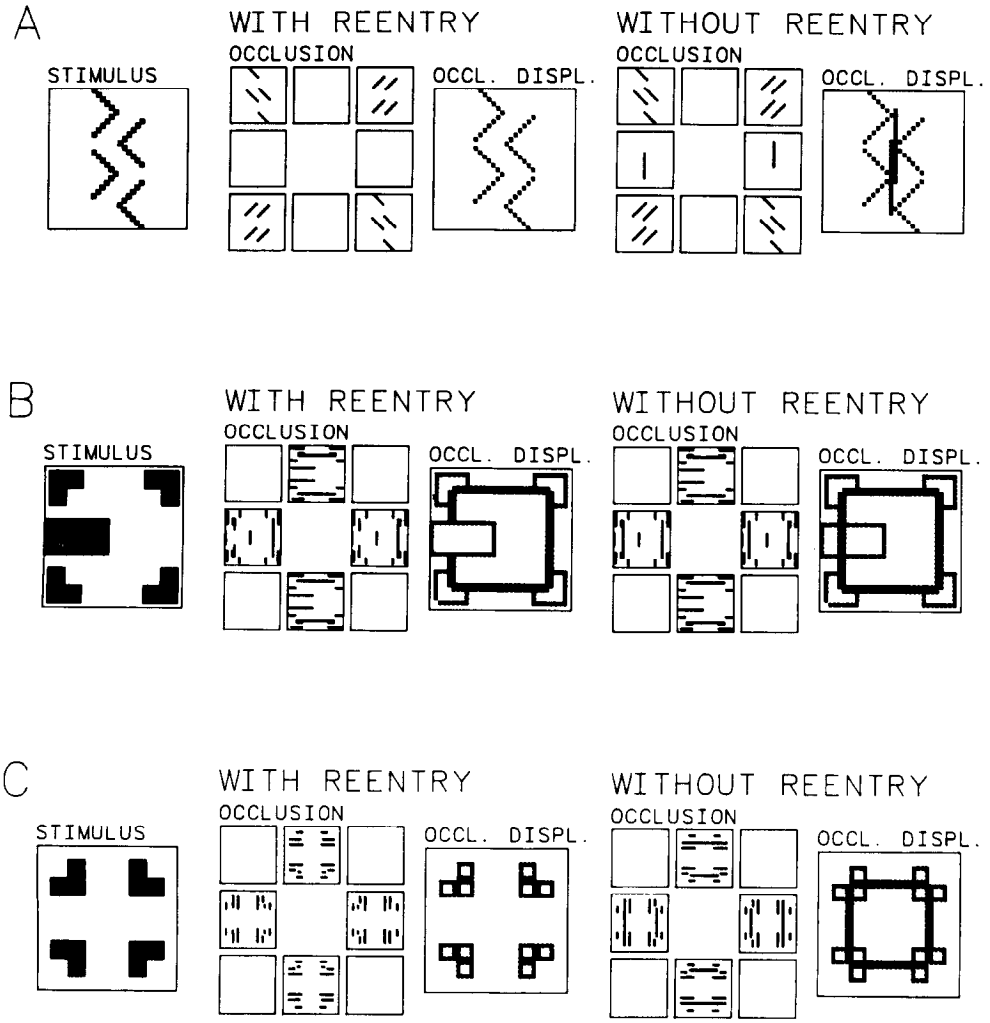

Figure 8. Conflict experiments. *A,* Response of Occlusion units to stimulus consisting of 4 angled vertices (Occlusion repertoires displayed in same convention as Fig. 4). In presence of connections from Common Termination Detectors to TD units (panels labeled "With Reentry") only responses to real contours are made. In the absence of these connections (panels on right labeled "Without Reentry") responses to vertical illusory contours are made. *B,* Responses to a stimulus consisting of an illusory square with occluding rectangle. In absence of reentrant connections from Occlusion to Reentrant Conflict repertoires (*right panels*), the illusory contour on the left side of the illusory square is discriminated as in Figure 7*C*. In presence of reentrant connections (*center panels*) illusory contour is censored at positions "behind" the occluding rectangle. *C,* Same elements as in illusory square stimulus (see Fig. 7*C*), with same line termination cues, but rearranged so that illusory square is not perceived by humans (see text). In absence of reentrant connections (*right*) networks generate illusory contours. In presence of reentry, illusory contours are censored between the 4 corner elements but not within the corner elements (see text).

nocellular"-based networks, which are chiefly concerned with relations between borders of objects, do not deal effectively with internal/external distinctions.

The examples of Figure 8 illustrate that the V_{OC} reentry system directly mediates the resolution of conflicts in the responses of different repertoires: in the absence of the reentrant connections, there is no inhibition of conflicting responses. Resolution of conflicts among areas has particular significance due to the fact that V_{OC} can generate contours based on reentrant inputs from *other* modality-selective centers, as we now discuss.

Structure-from-motion

The first example of cross-modal reentry involves the connections from V_{MO} to V_{OC}, which allow the system to use differential motion as a local cue to occlusion. Figure 9 shows the contours generated in response to a stimulus consisting of a central square region in which random dots are moved rightward at 1 pixel/cycle. This central square region is surrounded by a larger square region in which dots are moved to the left. Once the V_{MO} pathway has distinguished the directions of motion of the moving dots, the Direction Discontinuity units in V_{OC} (i.e., the directional equivalents of the Termination Discontinuity units) begin to respond to the local cues from regions of differential motion. The occlusion repertoires generate responses to colinear local cues, and over the next few iterations, these responses are sharpened, until they correspond to the borders between differentially moving dot fields. (See the Occlusion Display, which sums the responses of all 8 repertoires.) The exact locations of these generated contours fluctuate from cycle to cycle as the instantaneous positions of the random dots (and the gaps between them) change. In the absence of the V_{MO} to V_{OC} connections, there are no responses to the structure-from-motion contours (not shown).

As mentioned above, these contours are generated regardless of which directions the dots are moving in the 2 regions, as long as there is differential motion. Occlusion boundaries can be constructed to a wide range of geometrical configurations, and with multiple subregions of differential motion, including, for example, the 3-panel display shown in Figure 6.

Recursive synthesis of a combined illusion by means of reentry

The most critical test of cross-modal reentry in the present simulations involves the interaction of illusory contours and structure-from-motion in the combined illusion shown in Figure 10. The stimulus consists of 3 of the 4 corners used to make the illusory square in Figure 7*C*. However, in place of the fourth (lower-right) corner of the "illusory square," there are 2 fields of moving random dots: a square-shaped region and an inverse L-shaped region which fit together to make a larger square region. The random dots in the inverse L-shaped region move 1

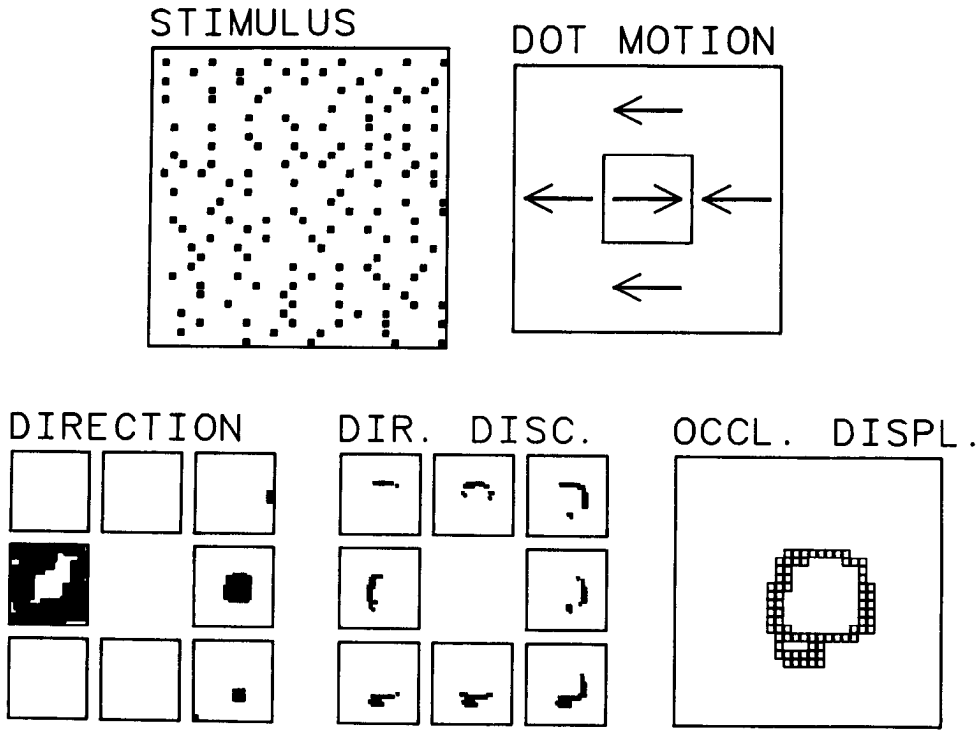

Figure 9. Cross-modal construction—the generation of structure-from-motion. Stimulus consisted of 1 pixel random dots moved eastward within a central square region and westward elsewhere in the array (see "Dot Motion") at 1 pixel/cycle. Responses of units after 5 cycles in the Direction and Direction Discontinuity (Dir. Disc.) repertoires (panels arranged by direction preference according to convention of Fig. 4). Direction units preferring eastward and westward motion respond to appropriate regions of dot motion. Direction discontinuity units generate borders between regions determined to contain differentially moving objects. Occlusion display shows (at larger scale) the superposed responses of the 8 Dir. Disc. repertoires. The exact positions of the structure-from-motion borders vary from cycle to cycle depending on variations in the gaps between random dots.

pixel/iteration to the right; those in the small square region move 1 pixel/iteration to the left (see panel labeled Dot Motion). The positions of the dots were determined using a random-number generator routine subject to the constraint that all dots must be separated by at least 3 pixels in the horizontal, vertical, and oblique directions.

Figure 10 shows the responses of units in the Direction, Direction Discontinuity, and Occlusion repertoires at 2 different times during presentation of the stimulus. As seen in the figure, by the second cycle, the Direction units discriminate the motion patterns, and the Occlusion repertoires generate responses to 2 sides of the illusory square. The reentrant connections between V_{MO} and V_{OC} begin to generate responses in the Direction Discontinuity repertoires to the structure-from-motion contours. Over the next few cycles, these responses are reentered back to "4B-Term" in V_{OR}. "4B-Term" repertoires act on these *reentrant* inputs in the same manner as upon normal *ascending* inputs from "4Cα" and detect terminations of the contours derived from structure-from-motion and illusory contours. The units responding to these terminations then activate the ascending V_{OC} pathway (see Fig. 1). Now, however, there are local (termination) cues for the construction of the remaining 2 sides of the illusory square, and these remaining contours are, in fact, produced, as shown in Figure 10 (cycle 4). Once generated, the contours are indefinitely stable. (Note that Fig. 4 shows the response of all repertoires in the system to the same stimulus used in Fig. 10.) We have tested this illusion on normal human subjects, and it is indeed perceived as an illusory square. The system works equally well with other directions of motion of the random-dot fields and other illusory shape configurations (triangles, etc.).

If the reentrant connections from the Occlusion to "4B-Term" units are cut, the necessary "cross-modal" interactions do not occur, and the bottom and right sides of the "illusory square" are not generated. The same negative result occurs if the V_{MO} to V_{OC} connections are cut (not shown).

Thus, an illusory figure, identical to that produced exclusively by the V_{OC} pathway, as shown in Figure 7*C*, can be produced through a *combination* of the action of the direct ascending V_{OC} pathway, the action of V_{OC} repertoires on inputs from the V_{MO} pathway, and the recursively reentered activity stimulated by these structure-from-motion contours acting on the V_{OC} pathway. The reentrant property of recursive synthesis thus generates one illusory construct (illusory contours) from another (structure-from-motion).

Discussion

The functional segregation of the visual cortex, as elucidated in recent years, has led to the view that individual cortical regions are more or less specialized for particular visual tasks, such as the discrimination of color, form, or motion (Zeki, 1978; Mishkin et al., 1983; Maunsell and Newsome, 1987; De Yeo and Van Essen, 1988; Livingstone and Hubel, 1988; Zeki and Shipp, 1988). This conclusion poses a central question: How are the operations of these segregated cortical areas integrated to produce the basis for a perceptually unified picture of the world? To provide a theoretical approach to this problem, we have used computer simulations to demonstrate how the properties of disparate visual maps can be integrated by processes of reentrant signaling. The RCI model provides a unitary explanation for a number of visual illusions involving interactions between multiple visual attributes (such as contour, depth, and motion) in terms of activation of reentrant pathways. In doing so, the model takes account of a dominant anatomical feature of the mammalian cortex—the massive systems of interareal corticocortical connections.

Any model of cortical integration must make certain implicit assumptions regarding the bases of perception. The present model

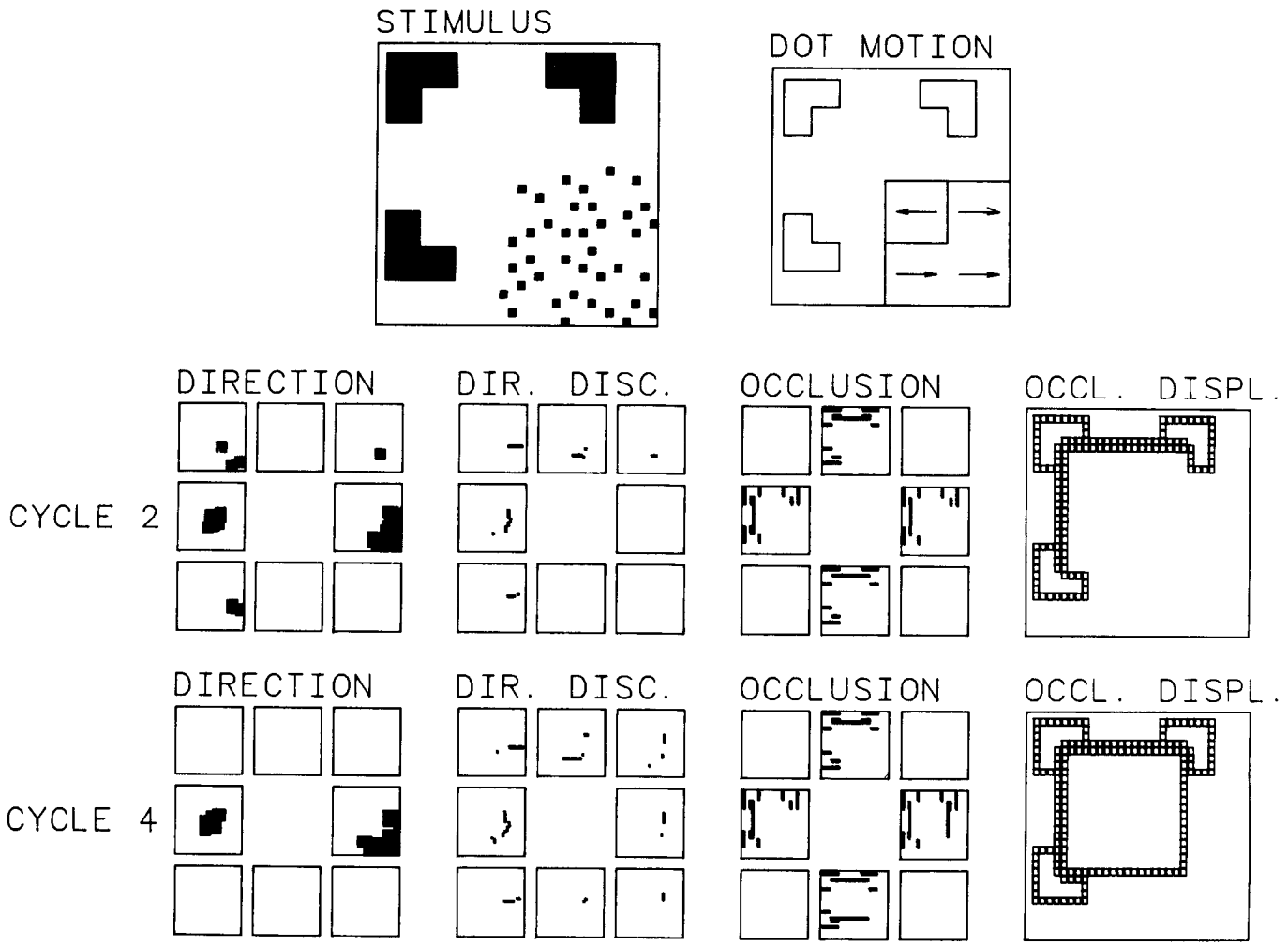

Figure 10. Recursive synthesis of a combined illusion. Responses of Direction, Direction Discontinuity (Dir. Disc.), and Occlusion repertoires to combined illusory contour and structure-from-motion stimulus. Stimulus consists of 3 of the 4 corner elements of Figure 7*C*. In place of bottom-right corner element is a random dot stimulus in which dots are moved at 1 pixel/cycle in the directions shown in panel labeled "Dot Motion." By the second cycle, the Occlusion repertoires have generated illusory contours between the corner elements (see Occl. Displ. for larger-scale view), the Direction units have begun to respond to the directions of dot motion, and the Direction Discontinuity units have generated structure-from-motion borders. By cycle 4, the responses to structure-from-motion borders have been reentered back to V_{OR} (see text), and their terminations have been detected and used by the ascending V_{OC} system to construct responses to the 2 remaining sides of an illusory square. These later illusory contours thus require the prior construction of borders due to structure-from-motion. Responses of other repertoires of this stimulus are shown in Figure 4.

suggests that the unitary nature of perception does not arise from a unitary locus of representation in higher cortical regions, but rather from the coordination (through reentry) of the operations of higher cortical areas with the more-or-less homomorphic representation of the signal world in primary visual cortex. The coherency of the cortical response is thus provided for by the coherency of the object itself as a source of signals.

Simulation experiments on reentry

The examples of reentrant connections used in these simulations are not exhaustive but were chosen to illustrate main principles. In the V_{MO} pathway, reentry significantly sharpens directional selectivity. The V_{OC} pathway contains 2 reentrant circuits. One reentrant pathway checks any generated construct against "reality" (i.e., inputs from the world) and resolves conflicts between the two. The other V_{OC} reentrant pathway allows responses to illusory contours generated in V_{OC} to be "recycled" back to V_{OR}, where they can be used in the construction of additional contours. Direct cross-modal reentry from V_{MO} to V_{OC} allows motion cues to be used for occlusion discriminations. Additional cross-modal reentry takes place when the effects of the V_{MO} to V_{OC} connections are reentered back to layer "4B" and then enter the ascending V_{OC} pathway. In these simulations, we have *not* included cross-modal back reentrant connections (i.e., V_{OC} to the V_{MO} projecting units in "4B" or V_{MO} to the V_{OC} projecting units), although connections that could carry out such reentry do exist in the monkey (Zeki and Shipp, 1988). We have also not included back reentry from V_{OR} to the LGN, despite the fact that this is one of the most striking reentrant systems in the CNS (Guillery, 1966), whose function has been the subject of considerable speculation (Singer, 1977; Anderson and Van Essen, 1987; Koch, 1987; Murphy and Sillito, 1987; Allman, 1988).

The multiple selectivities of the units in the simulated areas reflect a general cortical principle that can be called "functional degeneracy." Functional degeneracy is a mechanism by which

parallel systems can compensate for transient imbalances in the spatiotemporal distribution of tasks. An analogous situation exists in the distribution of tasks among communicating insect castes (Oster and Wilson, 1978), in which members of a caste specialized for one set of functions (e.g., workers) can, to certain extents, substitute in an emergency for members of another caste (e.g., soldiers). It is tempting to speculate that similar benefits accrue to the communicating areas of functionally segregated cortex.

Integration mechanisms

Part of the complexity in studying the coordination of cortical areas by reentry is due to the fact that different reentrant pathways can use different integrative mechanisms. The properties of several of these integrative mechanisms were demonstrated by tests of the system in the presence and the absence of reentry. The first mechanism involved the *resolution of conflicts* in the responses of different areas to the same stimulus (or conflicts within the same area to different aspects of the same stimulus). Such conflicts are unavoidable given that each area is more or less specialized for the discrimination of particular stimulus attributes. Figure 8 demonstrated several examples in which the responses of the V_{OC} occlusion repertoires to illusory contours conflicted with responses to other contours—either real or illusory. The reentrant circuit acted to "censor" the conflicting responses. Another example of conflict resolution involved the reentry between V_{MO} and V_{OR}. In that case, responses in V_{OR} are inhibited if they do not correspond to the true direction of motion as determined by V_{MO}.

The second mechanism of reentrant integration, *cross-modal construction,* allows one area to use the outputs of another area (which may be specialized for a different visual function) for its own operations. We showed how V_{OC} is able to use differential motion cues determined by V_{MO} to construct structure-from-motion boundaries. Several psychophysical analogs of cross-modal construction have been demonstrated in humans by Ramachandran (Ramachandran et al., 1973; Ramachandran and Cavanaugh, 1985; Ramachandran, 1986) in experiments showing how features determined through one submodality (e.g., disparity) interact with (or are "captured") by other features. For example, illusory contours can undergo apparent motion (Ramachandran et al., 1973), the perceived disparity of a background texture can be influenced by an overlying illusory surface (Ramachandran, 1986), apparent motion can "carry" a background texture along with it (Ramachandran and Cavanaugh, 1985), and the perceived location of a color border can be influenced by motion of a nearby illusory border. If we accept that some of these processes are carried out in separate cortical areas, then the psychophysical phenomenon of "capture" is a strong argument for the existence of reentry. In fact, Ramachandran has suggested that some of his observations may be carried out through connections between V1 and V2 (Ramachandran, 1986).

The third mechanism of integration, *recursive synthesis,* was exemplified by the reentrant pathways from V_{MO} and V_{OC} back to V_{OR}. These connections allow the outputs of a higher area to influence the *inputs* that it (or other higher areas) receive from lower areas. More importantly, recursive synthesis allows constructs derived in higher areas to be recycled to lower areas for use in the generation of additional constructs (where, by "construct," we mean patterned neuronal responses linked to invariant properties in the world).

Recursive synthesis provides the strongest *gedanken* argument for the existence of reentry in view of the fact that there are situations and responses that could not be accounted for in any other way. For example, even if units in V_{MO} (or correspondingly, V5) could *independently* construct responses to structure-from-motion, some kind of local recursive process would still be required to generate the contours shown in Figure 10. This is because the structure-from-motion contours must be generated *first* in order to provide the line-termination cues required for the illusory contours corresponding to the 2 missing sides of the illusory square. The most natural implementation for such a recursion, and one totally consistent with the known anatomy, is to let the connections from V_{OC} to "4B" reenter the responses to the illusory contours back to the early stages of the same pathway. There are numerous other examples of stimuli requiring such recursive processing (see Kanizsa, 1979).

Physiological basis of the simulations

The present simulations are not intended as a detailed model of the individual components of the extrastriate cortex of the monkey. Repertoires assigned to one simulated area could, in several cases, be assigned with equal justification to another. For example, the Wide Angle and Reentrant Conflict repertoires could have been assigned to V_{OR} or V_{OC} with equal plausibility. Moreover, properties that are generated by several separate units in the model could be generated *in vivo* by more complex integrative properties of single units, particularly given the nonlinear interactions possible within dendritic trees (Koch et al., 1982; Finkel and Edelman, 1985).

There are, of necessity, a number of *ad hoc* properties built into the RCI model (either due to lack of knowledge about the corresponding cortical mechanisms or the complexity of those that are known). There are 17 basic types of units used; the operations performed by these units fall into 5 physiological classes (see Table 2). Compared with the number of anatomically and physiologically defined visual cortical cell types (Dow, 1974; Van Essen, 1985; Kaas, 1986), these are relatively small numbers; however, they are nevertheless large numbers in the context of a model. We have found that multiple unit types are necessary, however, in order to generate appropriate responses to a wide range of illusory stimuli.

It is clear that many processes (from retinal to cognitive) may be involved in the normal visual functions and related visual illusions considered here, and it follows that any one model has little chance of accounting for all of the examples. However, the fact that humans perceive illusory contours after short (50 msec) presentations of the inducing stimulus (Reynolds, 1981) and that illusory contour perception can be inhibited if a masking stimulus is presented within 150 msec of the inducing stimulus (Petry and Gannon, 1987), is consistent with the time constants of corticocortical signaling along reentrant circuits. It has been estimated, for example, that the time delay between excitation of successively more central visual cortical areas by a peripheral stimulus is approximately 10 msec (Sereno, 1988). If one assumes a similar time delay for the reentrant pathway, then these psychophysically derived times would represent a few cycles of reentrant activity.

In this regard, it is important to note that, in the model, stable responses to a wide range of stimuli consistently appear within several cycles of simulation. Responses to illusory contours are generated on the first cycle of presentation, and responses to structure-from-motion are made within 4 or 5 cycles (depending

upon the fine-structure of the stimuli used), and occasionally by cycle 3.

Many of the basic properties of visual cortex are captured by the model; however, there are also a number of obvious shortcomings. Despite the drastic simplifications that have been made in the spatial and temporal structures of the receptive fields of simulated units (Shapley and Perry, 1986; Jones and Palmer, 1987), the orientation and directional tuning curves of Figure 5 are qualitatively similar (albeit with broader tuning) to those found in cat (Henry et al., 1974) and monkey (Hubel and Wiesel, 1977). The mechanism of temporally delayed inhibition that is responsible for the directional selectivity in "4Cα" and "4B-Dir" is similar, in principle, to that used in most models of directional selectivity (Barlow and Levick, 1965; Reichardt et al., 1983), and is in accord with the physiological evidence for the role of synaptic inhibition in directional selectivity (Orban, 1986). In the present model, the temporal delay is implemented in a novel way that was designed to emulate the production of an intracellular substance (e.g., a second messenger) that initiates an IPSP. We have achieved similar directional selectivity using other mechanisms, for example, a temporally delayed, heterosynaptic depression of synaptic efficacy.

Units in the simulated V_{MO} pathway share 2 important properties with cells in monkey V5: directional selectivity is best for small moving spots, and the receptive fields of the units are large compared with those in V_{OR}. Both of these properties reflect the constraints imposed by the "aperture problem" (Marr, 1982; Hildreth and Koch, 1987). Indeed, the V_{MO} pathway effectively overcomes the aperture problem, as responses to moving objects are largely independent of their orientation (see Fig. 5*C*).

The major shortcoming of the simulated V_{MO} pathway is the absence of a range of velocity selectivities (Maunsell and Van Essen, 1983; Newsome et al., 1986). In these simulations, velocity selectivity was limited to 1 pixel/iteration, and extension of this range would have required a proportionately larger number of units. Another shortcoming is the absence of large inhibitory surrounds or effects from beyond the classical receptive field (Allman et al., 1985). The capacity of cells in area MT (V5) to respond preferentially to *differential* motion between the center and periphery of their receptive fields (Allman et al., 1985) is ideally suited for use in the connections to V_{OC} mediating structure-from-motion. Use of units with these characteristics in the model might decrease the number of connections required since the necessary condition is differential motion, not the particular direction of motion followed on either side of a boundary.

We have provisionally identified simulated area V_{OC} with area V3 in the monkey; however, some of the properties of V_{OC} and its source units in "4B-Term" may, in fact, more closely correspond to those of area V2 or other cortical areas. The basis for identifying V_{OC} with V3 rests, in part, with the specialization of that cortical area for depth [cells in V3 are primarily binocular and selective for stereoptic disparity, although they are also, in general, activatable by monocular stimuli (Zeki, 1978; Poggio and Poggio, 1984; Poggio et al., 1985)]. In addition, as in the model, the overwhelming majority of cells in V3 are orientation selective (Zeki, 1978; Felleman and Van Essen, 1987). While not specifically implicating area V3, there is extensive psychophysical evidence that illusory contours are generated by the magnocellular system. For example, it has been found that illusory contours are not perceived under conditions that favor the parvocellular system, such as equiluminance and high spatial frequencies, and are perceived under conditions favoring the magnocellular system such as low luminance contrast (Livingstone and Hubel, 1987).

In the present model, V_{OC} responds to occlusion and illusory boundaries as well as to real boundaries. Thus, the distinction between real and constructed boundaries depends upon the lack of response to constructed boundaries in V_{OR} (and perhaps other cortical areas as well). The diaphanous, "unreal" quality of our perceptual sensation of illusory contours may be due to the fact that not all reentrantly connected visual cortical areas are activated in the same fashion as they are to nonillusory stimuli.

Other models

Figures 7–10 demonstrate that the V_{OC} pathway successfully generates responses to illusory contours and structure-from-motion when presented with several representative stimuli and that it does not generate these responses to control stimuli. The major assumption underlying the construction of the V_{OC} system is the scheme (shown in Fig. 3) of using local cues to occlusion as the "trigger features" for illusory contour generation. Most other models of illusory contour formation have taken a configuration of colinear lines separated by a gap as the "trigger feature." We have not used these "colinear" mechanisms in our scheme because we desired a single mechanism that, in addition to accounting for the results of Figure 7*C*, could also account for those of Figure 7*A* in which there are no such colinear cues. However, an attractive addition to the proposed mechanism would let such pairs of colinear lines (which need not be *exactly* colinear) prejudice the orientation of the initial segment of the generated contour. Such a mechanism may be necessary for the generation of curved illusory contours.

We have dealt exclusively with 2-dimensional stimuli, yet many of the most difficult and important problems in visual perception arise when depth is added. For example, structure-from-motion [and the related kinetic-depth effect (Ullman, 1979)] can create 3-dimensional shapes, and several interesting models have attacked this problem (Zucker, 1986; Siegel and Anderson, 1988). We have concentrated on the detection of straight lines; however, it is well known that curved illusory contours are readily perceived (Kanizsa, 1979). The major power of Ullman's (1976) model is its ability to handle both straight and curved contours. More recently, Zucker and his colleagues (Zucker, 1986; Dobbins et al., 1987) have presented theoretical and experimental evidence that end-stopped cells may primarily respond to curvature (Hubel and Wiesel, 1977). In this regard, our V_{OC} pathway, which receives inputs from asymmetric end-stopped units, may be able to be generalized to produce curved contours.

As mentioned above, the ascending V_{OC} pathway shares several common elements with the scheme proposed by Baumgartner and his colleagues (Baumgartner et al., 1984; von der Heydt et al., 1984; Peterhans et al., 1986). The critical similarity is the use of units constructed to detect colinear line terminations (as opposed to colinear *lines*, as used in most models designed to detect illusory contours). The present model differs in that (1) it is based on the principle that occlusion is the fundamental construct, regardless of the modality of the cues; (2) it contains extensive reentrant circuitry that checks for conflicts with real lines and allows cross-modal interactions with the motion system; (3) it contains units (Occlusion units) that actually generate the illusory contours; (4) it considers multiple possible orientations of lines; and (5) it requires that terminations approach an occlusion border from both sides. Based on their recordings

from V2 (Peterhans et al., 1986), Baumgartner's scheme only requires terminations approaching from a single side. However, in that case, the illusory square stimulus (see Fig. 7*C*) would give rise to spurious illusory contours along the outside edges of the square. From a larger point of view, however, the present simulations support the basic scheme proposed by Baumgartner and his colleagues.

Grossberg and Mingolla (1985) and Grossberg (1987) have proposed explanations for a wide range of visual illusions using a model consisting of 2 distributed parallel systems: one concerned with defining boundaries and the other with filling-in the interiors of objects. They consider the problem of illusory contours and propose a mechanism that bears certain similarities to the present scheme, in particular, the use of return connections to amplify particular responses. However, there are a number of important differences between the proposals: (1) Grossberg and Mingolla do not emphasize the centrality of occlusion as the basis of illusory contours, (2) they postulate separate mechanisms to account for illusory contours that are parallel versus perpendicular to edges (we postulate a single process—see Fig. 7, *A, C*), (3) their illusory contours are generated in a discontinuous, iterative process in which the midpoints of gaps are successively filled-in (our process is 1-step and parallel), (4) their proposed cellular mechanisms are not related to those in the nervous system, and (5) there has been no extensive testing of their model through large-scale simulations.

Kanizsa (1979) has argued that illusory figures of the kind discussed here demonstrate the principle of Prägnanz developed by the Gestalt psychologists (Koffka, 1935; Beck, 1982). In fact, reentry among multiple, functionally segregated cortical areas may give rise to something like Prägnanz in that the constraints of each area are weighed in a cooperative and competitive process of figural synthesis. Kanizsa has also emphasized the importance of constructing "amodal contours" (those corresponding to the occluded object) in explaining human perceptions of a range of illusory contour phenomena (Kanizsa, 1979). We have not studied this aspect of the problem inasmuch as it was not necessary to generate responses to the occlusion boundaries used here.

Extensions of the model

A major area of extension of the present model would be to consider the temporal factors involved in reentrant signaling (Edelman, 1981). One mechanism that may aid in the coordination and synchronization of local operations in various regions is the observation that cells in the same orientation column may fire in a correlated and phase-locked manner (Gray and Singer, 1989). Such fast temporal organization of the response of cells within a neuronal group may allow reentrantly connected groups to mutually entrain each others' activity, as has been shown in a recent simulation (Sporns et al., 1989). Another obvious extension of the model is to consider interactions with the parvocellular system and problems concerned with color and the "filling in" of the interior of an object.

The results of the present simulations of the RCI model lead to a number of falsifiable experimental predictions.

1. Single cells will be found in the cortex that respond to oriented lines formed by all of the following conditions: (a) luminance boundaries, (b) occlusion boundaries, (c) illusory contours, and (d) structure-from-motion. The same cells will also most likely respond to oriented boundaries defined by color, texture, or disparity differences.

2. Ablation or pharmacological inactivation of a cortical area corresponding to simulated area V_{OC} should destroy the response to illusory contours found in other extrastriate areas, including contours generated via structure-from-motion. Certain other higher cortical areas may also play critical roles in this process and may show similar effects after inactivation.

3. Ablation or pharmacological inactivation of cortical area V5 (or the area corresponding to simulated area V_{MO}) should destroy structure-from-motion in area V3 (or the cortical area corresponding to simulated area V_{OC}) without affecting illusory contour formation from line termination stimuli.

4. The role of particular cortical areas in figural synthesis may be demonstrated with experiments analogous to those using equiluminant stimuli to isolate the role of the magnocellular system (Livingstone and Hubel, 1988). For example, structure-from-motion can be generated with stimuli moving at high velocities that are beyond the range of all cells except those in V5. Additional stimuli can be constructed that must necessarily involved a particular area, for example, subtle stereoscopic disparity cues requiring V3. A recursive synthesis experiment combining 2 of these stimuli would strongly argue for a necessary role of reentrant signaling within the magnocellular pathway.

5. The recursive aspects of reentry may be detected by using poststimulus time histograms to analyze the response of cells in V3, or the analog of simulated area V_{OC}, to combined illusions, such as that shown in Figure 10. The response to the recursively generated contours (bottom and left side of illusory square in Fig. 10) will be delayed (by at least 20 msec) with respect to response of the same cell to illusory contours (e.g., the illusory square of Fig. 7*C* of the same size and position), occluded contours, or a real luminance border.

In conclusion, in the present computer simulation studies of the RCI model, we have provided a constructive example illustrating the role of reentry in the integration of distributed cortical systems. The understanding of this fundamental cortical process will require the convergence of simulation studies with anatomical, physiological, and psychophysical experiments to check the complex transactions leading to coordinated function. Elaboration of the principles governing reentrant networks could then be fruitfully applied to numerous other multimodal and associational pathways of the cortex.

References

Albright, T. D. (1984) Direction and orientation selectivity of neurons in visual area MT of the macaque. J. Neurophysiol. *52:* 1106–1130.

Allman, J. (1988) Variations in visual cortex organization in primates. In *Neurobiology of Neocortex,* P. Rakic and W. Singer, eds., pp. 29–40, Wiley, New York.

Allman, J. M., and J. H. Kaas (1971) Representation of the visual field in striate and adjoining cortex of the owl monkey. Brain Res. *35:* 89–106.

Allman, J., F. Miezin, and E. McGuinness (1985) Stimulus specific responses from beyond the classical receptive field: Neurophysiological mechanisms for local-global comparisons in visual neurons. Annu. Rev. Neurosci. *8:* 407–430.

Anderson, C. H., and D. C. Van Essen (1987) Shifter circuits—a computational strategy for dynamic aspects of visual processing. Proc. Natl. Acad. Sci. USA *84:* 6297–6301.

Ballard, D. H., G. E. Hinton, and T. J. Sejnowski (1983) Parallel visual computation. Nature *306:* 21–26.

Barlow, H. B., and R. W. Levick (1965) The mechanism of directional selectivity in the rabbit's retina. J. Physiol. (Lond.) *173:* 477–504.

Baumgartner, G., R. von der Heydt, and E. Peterhans (1984) Anomalous contours: A tool in studying the neurophysiology of vision. Exp. Brain Res. Suppl. *9:* 413–419.

Beck, J. (1982) *Organization and Representation in Perception,* Lawrence Erlbaum, Hillsdale, NJ.

Blakemore, C., R. H. S. Carpenter, and M. A. Georgeson (1970) Lateral inhibition between orientation detectors in the human visual system. Nature *228:* 37–39.

Burkhalter, A., D. J. Felleman, W. T. Newsome, and D. C. Van Essen (1986) Anatomical and physiological asymmetries related to visual areas V3 and VP in macaque extrastriate cortex. Vision Res. *26:* 63–80.

Coren, S. (1972) Subjective contour and apparent depth. Psychol. Rev. *79:* 359–367.

DeYeo, E. A., and D. C. Van Essen (1988) Concurrent processing streams in monkey visual cortex. Trends Neurosci. *11:* 219–226.

Dobbins, A., S. W. Zucker, and M. S. Cynader (1987) Endstopping in the visual cortex as a neural substrate for calculating curvature. Nature *329:* 438–441.

Dow, B. (1974) Functional classes of cells and their laminar distribution in monkey visual cortex. J. Neurophysiol. *37:* 927–946.

Edelman, G. M. (1978) Group selection and phasic reentrant signalling: A theory of higher brain function. In *The Mindful Brain,* G. M. Edelman and V. B. Mountcastle, eds., pp. 51–100, MIT Press, Cambridge, MA.

Edelman, G. M. (1981) Group selection as the basis for higher brain function. In *Organization of the Cerebral Cortex,* F. O. Schmidt, F. G. Worden, G. Adelman, and S. G. Dennis, eds., pp. 535–563, MIT Press, Cambridge, MA.

Edelman, G. M. (1987) *Neural Darwinism,* Basic Books, New York.

Edelman, G. M., and L. H. Finkel (1984) Neuronal group selection in the cerebral cortex. In *Dynamic Aspects of Neocortical Function,* G. M. Edelman, W. E. Gall, and W. M. Cowan, eds., pp. 653–695, Wiley, New York.

Felleman, D. J., and D. C. Van Essen (1987) Receptive field properties of neurons in area V3 of macaque monkey extrastriate cortex. J. Neurophysiol. *57:* 889–920.

Ferster, D. (1987) Origin of orientation-selective EPSPs in simple cells of cat visual cortex. J. Neurosci. *7:* 1780–1791.

Finkel, L. H., and G. M. Edelman (1985) Interaction of synaptic modification rules within populations of neurons. Proc. Natl. Acad. Sci. USA *82:* 1291–1295.

Gilbert, C. D. (1977) Laminar differences in receptive field properties of cells in cat primary visual cortex. J. Physiol. (Lond.) *268:* 391–421.

Gilbert, C. D., and J. P. Kelly (1975) Projections of cells in different layers of cat visual cortex. J. Comp. Neurol. *163:* 81–105.

Gray, C. M., and W. Singer (1989) Neuronal oscillations in orientation columns of cat visual cortex. Proc. Natl. Acad. Sci. USA *86:* 1698–1702.

Gregory, R. (1972) Cognitive contours. Nature *238:* 51–52.

Grossberg, S. (1987) Cortical dynamics of three-dimensional form, color, and brightness perception: I. Monocular theory. Percept. Psychophys. *41:* 87–116.

Grossberg, S., and E. Mingolla (1985) Neural dynamics of form perception: Boundary completion, illusory figures, and neon color spreading. Psychol. Rev. *92:* 173–211.

Guillery, R. W. (1966) Patterns of fiber degeneration in the dorsal lateral geniculate nucleus of the cat following lesions in the visual cortex. J. Comp. Neurol. *130:* 197–220.

Henry, G. H., B. Dreher, and P. O. Bishop (1974) Orientation specificity of cells in cat striate cortex. J. Neurophysiol. *37:* 1394–1409.

Hildreth, E. C., and C. Koch (1987) The analysis of visual motion: From computational theory to neuronal mechanisms. Annu. Rev. Neurosci. *10:* 477–533.

Hubel, D. H., and T. N. Wiesel (1962) Receptive fields, binocular interaction and functional architecture in the cat's visual cortex. J. Physiol. (Lond.) *160:* 106–154.

Hubel, D. H., and T. N. Wiesel (1977) Functional architecture of the macaque monkey visual cortex. Proc. R. Soc. London [Biol.] *198:* 1–59.

Jones, J. P., and L. A. Palmer (1987) The two-dimensional spatial structure of simple receptive fields in cat striate cortex. J. Neurophysiol. *58:* 1187–1211.

Kaas, J. H. (1986) The structural basis for information processing in the primate visual system. In *Visual Neuroscience,* J. D. Pettigrew, K. J. Sanderson, and W. R. Levick, eds., pp. 121–141, Cambridge U. P., New York.

Kanizsa, G. (1979) *Organization in Vision,* Praeger, New York.

Kienker, P. K., T. J. Sejnowski, G. E. Hinton, and L. E. Schumacher (1986) Separating figure from ground with a parallel network. Perception *15:* 197–216.

Koch, C. (1987) The action of the corticofugal pathway on sensory thalamic nuclei: A hypothesis. Neuroscience *23:* 399–406.

Koch, C., T. Poggio, and V. Torre (1982) Retinal ganglion cells: A functional interpretation of dendritic morphology. Phil. Trans. R. Soc. Lond. [Biol.] *298:* 227–264.

Koffka, K. (1935) *Principles of Gestalt Psychology,* Harcourt, Brace, New York.

Livingstone, M. S., and D. H. Hubel (1987) Psychophysical evidence for separate channels for the perception of form, color, movement, and depth. J. Neurosci. *7:* 3416–3468.

Livingstone, M., and D. Hubel (1988) Segregation of form, color, movement, and depth: Anatomy, physiology, and perception. Science *240:* 740–749.

Marr, D. (1982) *Vision: A Computational Investigation into the Human Representation and Processing of Visual Information,* W. H. Freeman, San Francisco.

Maunsell, J. H. R., and W. T. Newsome (1987) Visual processing in monkey extrastriate cortex. Annu. Rev. Neurosci. *10:* 363–401.

Maunsell, J. H. R., and D. C. Van Essen (1983) Functional properties of neurons in middle temporal visual area of the macaque monkey. I. Selectivity for stimulus direction, speed, and orientation. J. Neurophysiol. *49:* 1127–1147.

Merzenich, M., G. Recanzone, W. M. Jenkins, T. T. Allard, and R. J. Nudo (1988) Cortical representation plasticity. In *Neurobiology of Neocortex,* P. Rakic and W. Singer, eds., pp. 41–68, Wiley, New York.

Mishkin, M., L. G. Ungerleider, and K. A. Macko (1983) Object vision and spatial vision: Two cortical pathways. Trends Neurosci. *6:* 414–417.

Mountcastle, V. B. (1978) An organizing principle for cerebral function: The unit module and the distributed system. In *The Mindful Brain,* G. M. Edelman and V. B. Mountcastle, eds., pp. 7–50, MIT Press, Cambridge, MA.

Movshon, J. A., E. H. Adelson, M. S. Grizzi, and W. T. Newsome (1985) The analysis of moving visual patterns. Exp. Brain Res. (Suppl. *11*): 117–151.

Murphy, P. C., and A. M. Sillito (1987) Corticofugal feedback influences the generation of length tuning in the visual pathway. Nature *329:* 727–729.

Nakayama, K., and G. H. Silverman (1986) Serial and parallel processing of visual feature conjunctions. Nature *320:* 264–265.

Newsome, W. T., A. Mikami, and R. H. Wurtz (1986) Motion selectivity in macaque visual cortex. III. Psychophysics and physiology of apparent motion. J. Neurophysiol. *55:* 1340–1351.

Orban, G. A. (1986) Processing of moving images in the geniculocortical pathway. In *Visual Neuroscience,* J. D. Pettigrew, K. J. Sanderson, and W. R. Levick, eds., pp. 121–141, Cambridge U. P., New York.

Oster, G. F., and E. O. Wilson (1978) *Caste and Ecology in the Social Insects,* Princeton U. P., Princeton, NJ.

Pearson, J. C., L. H. Finkel, and G. M. Edelman (1987) Plasticity in the organization of adult cerebral cortical maps: A computer simulation based on neuronal group selection. J. Neurosci. *7:* 4209–4223.

Peterhans, E., R. von der Heydt, and G. Baumgartner (1986) Neuronal responses to illusory contour stimuli reveal stages of visual cortical processing. In *Visual Neuroscience,* J. D. Pettigrew, K. J. Sanderson, and W. R. Levick, eds., pp. 343–352, Cambridge U. P., Cambridge, UK.

Peters, A. (1987) Number of neurons and synapses in primary visual cortex. In *Cerebral Cortex, Vol. 6: Further Aspects of Cortical Function Including Hippocampus,* E. G. Jones and A. Peters, eds., pp. 267–294, Plenum, New York.

Petry, S., and R. Gannon (1987) Time, motion, and objectness in illusory contours. In *The Perception of Illusory Contours,* S. Petry and G. E. Meyer, eds., pp. 193–200, Springer-Verlag, New York.

Poggio, G. F., and T. Poggio (1984) The analysis of stereopsis. Annu. Rev. Neurosci. *7:* 379–412.

Poggio, G. F., B. C. Motter, S. Squatrito, and Y. Trotter (1985) Responses of neurons in visual cortex (V1 and V2) of the alert macaque to dynamic random-dot stereograms. Vision Res. *25:* 397–406.

Ramachandran, V. S. (1986) Capture of stereopsis and apparent motion by illusory contours. Percept. Psychophys. *39:* 361–373.

Ramachandran, V. S., and P. Cavanaugh (1985) Subjective contours capture stereopsis. Nature *317:* 527–530.

Ramachandran, V. S., V. M. Rao, and T. R. Vidyasagar (1973) Apparent movement with subjective contours. Vision Res. *13:* 1399–1401.

Reeke, G. N., Jr., and G. M. Edelman (1987) Selective neural networks and their implications for recognition automata. Int. J. Supercomputer Appl. *1:* 44–48.

Reichardt, W., T. Poggio, and K. Hausen (1983) Figure-ground discrimination in the visual system of the fly. Part II. Towards the neural circuitry. Biol. Cybernet. *46:* 1–30.

Reynolds, R. (1981) Perception of an illusory contour as a function of processing time. Perception *10:* 107–115.

Rockland, K. S., and D. N. Pandya (1979) Laminar origins and terminations of cortical connections of the occipital lobe in the rhesus monkey. Brain Res. *179:* 3–20.

Sereno, M. I. (1988) The visual system. In *Organization of Neural Networks,* W. von Seelen, G. Shaw, and U. M. Leinhos, eds., pp. 167–184, VCH Publishers, New York.

Shapley, R., and V. H. Perry (1986) Cat and monkey retinal ganglion cells and their visual functional roles. Trends Neurosci. *9:* 229–235.

Siegel, R. M., and R. A. Anderson (1988) Perception of three-dimensional structure from motion in monkey and man. Nature *331:* 259–261.

Singer, W. (1977) Control of thalamic transmission by corticofugal and ascending reticular pathways in the visual system. Physiol. Rev. *57:* 386–420.

Sporns, O., J. A. Gally, G. N. Reeke, and G. M. Edelman (1989) Reentrant signaling among simulated neuronal groups leads to coherency in their oscillatory activity. Proc. Natl. Acad. Sci. USA (in press).

Stevens, K. A. (1981) Evidence relating subjective contours and interpretations involving occlusion. A. I. Memo 637, MIT Artificial Intelligence Laboratory.

Tigges, J., M. Tigges, and A. A. Perachio (1977) Complementary laminar terminations of afferents to area 17 originating in area 18 and in lateral geniculate nucleus in squirrel monkey. J. Comp. Neurol. *176:* 87–100.

Ullman, S. (1976) Filling-in the gaps: The shape of subjective contours and a model for their generation. Biol. Cybernet. *25:* 1–6.

Ullman, S. (1979) *The Interpretation of Visual Motion.* MIT Press, Cambridge, MA.

Van Essen, D. C. (1985) Functional organization of primate visual cortex. In *Cerebral Cortex, Vol. 3: Visual Cortex,* A. Peters and E. Jones, eds., pp. 259–320, Plenum, New York.

van Tuijl, H. F. J. M. (1975) A new visual illusion: Neonlike color spreading and complementary color induction between subjective contours. Acta Psychol. *39:* 441–445.

von der Heydt, R., E. Peterhans, and G. Baumgartner (1984) Illusory contours and cortical neuron responses. Science *224:* 1260–1262.

Wiener, N. (1948) *Cybernetics,* MIT Press, Cambridge.

Zeki, S. M. (1969) Representation of central visual fields in prestriate cortex of monkey. Brain Res. *14:* 271–291.

Zeki, S. M. (1971) Cortical projections from two prestriate areas in the monkey. Brain Res. *34:* 19–35.

Zeki, S. M. (1978) Functional properties in visual cortex of rhesus monkey. Nature *274:* 423–428.

Zeki, S. M., and S. Shipp (1988) The functional logic of cortical connections. Nature *335:* 311–317.

Zucker, S. W. (1986) The computational connection in vision: Early orientation selection. Behav. Res. Methods Instrum. Comput. *18:* 608–617.